nature protocols

PROTOCOL

https://doi.org/10.1038/s41596-023-00831-w

Check for updates

Ex vivo immunocapture and functional characterization of cell-type-specific mitochondria using MitoTag mice

Natalia Prudente de Mello[1,2,3,7], Caroline Fecher[1,3,4,7], Adrian Marti Pastor[1], Fabiana Perocchi[1,2,5,8]✉ and Thomas Misgeld[1,5,6,8]✉

Mitochondria are key bioenergetic organelles involved in many biosynthetic and signaling pathways. However, their differential contribution to specific functions of cells within complex tissues is difficult to dissect with current methods. The present protocol addresses this need by enabling the ex vivo immunocapture of cell-type-specific mitochondria directly from their tissue context through a MitoTag reporter mouse. While other available methods were developed for bulk mitochondria isolation or more abundant cell-type-specific mitochondria, this protocol was optimized for the selective isolation of functional mitochondria from medium-to-low-abundant cell types in a heterogeneous tissue, such as the central nervous system. The protocol has three major parts: First, mitochondria of a cell type of interest are tagged via an outer mitochondrial membrane eGFP by crossing MitoTag mice to a cell-type-specific Cre-driver line or by delivery of viral vectors for Cre expression. Second, homogenates are prepared from relevant tissues by nitrogen cavitation, from which tagged organelles are immunocaptured using magnetic microbeads. Third, immunocaptured mitochondria are used for downstream assays, e.g., to probe respiratory capacity or calcium handling, revealing cell-type-specific mitochondrial diversity in molecular composition and function. The MitoTag approach enables the identification of marker proteins to label cell-type-specific organelle populations in situ, elucidates cell-type-enriched mitochondrial metabolic and signaling pathways, and reveals functional mitochondrial diversity between adjacent cell types in complex tissues, such as the brain. Apart from establishing the mouse colony (6–8 weeks without import), the immunocapture protocol takes 2 h and functional assays require 1–2 h.

Introduction

Mainly known as the cell's powerhouses[1], mitochondria have pleiotropic roles essential for cellular and organismal life in virtually all eukaryotes. Importantly, most mitochondrial functions including energy metabolism, signaling, redox homeostasis, and cell death are tailored to the physiological demands of each organ and remodel during development and disease states[2–5]. This often results in surprisingly specific cellular phenotypes that cannot easily be modeled in vitro. Yet, whether tissue-specific mitochondrial diversity is due to the general metabolic state of an organ or reflects differences in cell-type-specific mitochondrial proteomes and their regulation, remains an open question. This led us to devise a tool to systematically explore cell-type-specific differences in mitochondrial metabolism and the underlying organelle's proteome. For this, we[6] and others[7] introduced the MitoTag approach that enables the cell-type-specific genetic tagging and isolation of mitochondria from a mouse tissue of interest.

Here, we provide an in-depth protocol of the MitoTag workflow (Fig. 1) that allows users to (1) generate and validate a cell-type-specific MitoTag mouse line via intercrossing of a 'flox-stopped' MitoTag line with suitable cell-type-specific Cre-driver lines, which enables the expression of an outer mitochondrial membrane eGFP (GFP-OMM) in the cell type of interest (Box 1), (2) isolate intact and functional mitochondria directly from their in vivo tissue context via a high-affinity magnetic immunocapture (IC) strategy (Figs. 2–4), and (3) interrogate functional properties of immunocaptured

[1]Institute of Neuronal Cell Biology, Technical University of Munich, Munich, Germany. [2]Institute for Diabetes and Obesity, Helmholtz Zentrum München, Munich, Germany. [3]Graduate School of Systemic Neurosciences, Ludwig-Maximilians Universität München, Munich, Germany. [4]Department of Cell Biology & Physiology, School of Medicine, Washington University in St Louis, St Louis, MO, USA. [5]Munich Cluster for Systems Neurology, Munich, Germany. [6]German Center for Neurodegenerative Diseases, Munich, Germany. [7]These authors contributed equally: Natalia Prudente de Mello, Caroline Fecher. [8]These authors jointly supervised this work: Fabiana Perocchi, Thomas Misgeld. ✉e-mail: fabiana.perocchi@helmholtz-muenchen.de; thomas.misgeld@tum.de

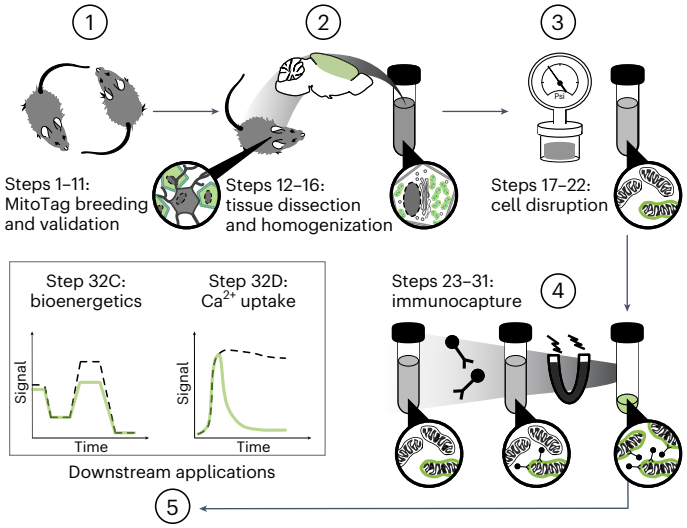

Fig. 1 | Workflow for the isolation of cell-type-specific mitochondria. Step numbers correspond to those in the 'Procedure' section. Stage 1: MitoTag mice are intercrossed with Cre-driver lines to achieve GFP-OMM expression in a cell type of interest (Steps 1–3), after which expression patterns are validated (Steps 4–11). Stage 2: the tissue of interest is dissected and homogenized to a single-cell suspension (Steps 12–16). Stage 3: mitochondria are released from cells via nitrogen decompression and nuclei and cell debris are removed by centrifugation (Steps 17–22). Stage 4: the post-nuclear lysate is incubated with magnetic beads coated with antibodies against GFP, and tagged mitochondria are magnetically separated from untagged organelles and other cellular components via immunocapture (Steps 23–31). Stage 5: cell-type-specific mitochondria are pelleted and can be used for downstream applications, such as mitochondrial bioenergetics with the Seahorse analyzer (Steps 32C) or Ca^{2+} uptake assays (Steps 32D).

mitochondria such as oxidative phosphorylation and calcium (Ca^{2+}) uptake ex vivo (Figs. 5–7). Our protocol was optimized to characterize mitochondrial diversity across the central nervous system (CNS), a tissue with a highly heterogeneous composition of cell types. We also provide advice on how to adapt the MitoTag protocol to other tissues, cell types and downstream applications (Box 2). The exact type of targeted analyses will determine the amount of starting tissue, the nature of required controls and the details of the IC strategy.

Development of the protocol

A growing number of mitochondrial functions can be directly monitored in vivo using genetically encoded metabolic sensors[8], but ex vivo organelle profiling remains confined to bulk mitochondrial fractions isolated from whole tissues. Standard purification methods for mitochondria are not cell-type specific and thus are unable to capture mitochondrial diversity within a tissue. Predicting cell-type-specific mitochondrial proteomes from transcriptomes is challenging, more than for other organelles, given that their biogenesis depends on transcription from two genomes, local translation and protein import across two membranes, and a multilayered quality control system[9]. Moreover, mitochondrial dynamics throughout the cell's geometry generate distinct organelle subpopulations, for example, in neuronal dendrites and axons[10,11]. Indeed, the lifetime of mitochondrial proteins span from minutes to months, suggesting variable dependence of protein levels on instantaneous somatic transcription[12].

Inspired by the success of reporter mouse lines for genetic organelle tagging (e.g. RiboTag mice[13]), as well as for fast and gentle isolation of mitochondria that can be achieved by magnetic bead isolation in vitro[14], we first engineered a reporter mouse for the tagging of cell-type-specific mitochondria and an IC protocol for their isolation and subsequent ex vivo profiling. Horie et al.[15] previously reported on a chimeric protein consisting of eGFP fused to the C-terminal 37 amino acids of OMP25 (also known as SYNJ2BP). This construct, termed GFP-OMM, which is devoid of functional domains of OMP25, is properly inserted into the outer mitochondrial membrane facing the eGFP towards the cytosol. Such a handle is suitable for IC of mitochondria from cells[16] without affecting their functionality, and its fluorescent properties allow direct confirmation of cell-type specificity, organelle distribution, morphology and dynamics via microscopy. Therefore, we generated a *Rosa26* knock-in mouse line (named MitoTag) by inserting GFP-OMM into an expression cassette containing a *loxP* site-flanked stop element, which silences the CAG promoter-dependent expression

Box 1 | Breeding of MitoTag mice with Cre-driver lines and mouse disease models

The MitoTag mouse model is a *Rosa26* knock-in reporter mouse that harbors an expression cassette containing the CAG promoter, a *loxP*-flanked stop cassette and GFP-OMM (Extended Data Fig. 1a). Use of the *Rosa26* gene locus on chromosome 6 is a common genetic strategy in mice, given that this locus is ubiquitously expressed in most cells[65] and hence, has been used by researchers for the conditional expression of fluorescent proteins and sensors[66]. GFP-OMM is an outer mitochondrial membrane eGFP tag facing towards the cytosol. In nonrecombined mice, GFP-OMM expression is prevented by the *loxP*-flanked stop cassette. When MitoTag mice are bred with Cre-driver lines, the *loxP*-flanked stop cassette is excised from the genome via the enzyme Cre recombinase, and GFP-OMM is expressed in the recombined cells and their daughter cell lineages. The timing of Cre induction is critical (Table 1 and Extended Data Fig. 2): Cre expression too early during embryonic development leads to recombination in blastocysts, stem cells or progenitor cells (Extended Data Fig. 2c), which results in whole-animal or -tissue recombination, respectively. By contrast, Cre induction in adult mice can be sparse due to the limited accessibility of all cells of a given cell type (e.g., neuronal subtypes in the brain). See, for example, Extended Data Fig. 2e, in which MitoTag expression is enabled via the Cre-driver line Plp1-cre/ERT with tamoxifen administration in adult mice. Here, we observed sparse labeling of astrocytes in cerebellum and no oligodendrocyte labeling, which would be the expected target cell type.

While genetically there is no difference between the recombined MitoTag loci in two crossings with different Cre-driver lines, we have observed fluorescence intensity differences in GFP-OMM between different cell types (e.g., astrocytes and neurons)[6]. The reasons for these differences are not clear, but rather than indicating variable efficiency of the *Rosa26* locus-integrated CAG promoter across cell types, the differential brightness of GFP-OMM could also be linked to differences in protein dilution due to cell size, OMM protein import and turnover, or simply distinct mitochondrial geometries. No obvious GFP-OMM fluorescence differences have been observed within the same Cre-driver line crossing or the same cell type with different Cre-driver lines. In our experience, using homozygote MitoTag mice does not improve IC yield, while increased GFP levels can be detected in western blots.

We have delivered Cre recombinase in two ways: (i) via intercrossing with mouse Cre-driver lines (Step 3A) or (ii) via transduction with viral vectors (Step 3B). In both cases, a cell-type-specific promoter drives the expression of Cre recombinase and restricts the excision of the stop cassette to this cell type. By contrast, Cre recombinase negative cells of the same mouse retain the stop cassette and do not express GFP-OMM. There are certain advantages and disadvantages to both strategies. Intercrossing with Cre-driver lines allows for a broader expression of GFP-OMM in a given cell type (close to 100%) and a more consistent expression phenotype between experimental animals. Due to the common use of Cre-driver lines for conditional gene deletions in mice, a large number of mouse lines exist and are distributed via repositories (e.g., The Jackson Laboratory, MMRRC, MGI). The primary publication or repository characterization should be consulted for cell-type specificity and timing of Cre recombinase expression. However, option (i) requires substantial breeding capacities and time. Also, some Cre-driver lines can only be maintained as heterozygous mice and/or crossing is restricted to one sex (e.g., because of expression in germ cells). It is known that the expression patterns of Cre-driver lines can change over time, e.g., due to genetic drift[49].

The use of viral vectors, option (ii), eliminates the need for extensive breeding given that all offspring can be used if homozygous MitoTag mice are crossed to wild-type mice. However, the neonatal injection of viral vectors adds an invasive procedure and requires specific approval by the Institutional Animal Care and Use Committee (IACUC), as well as access to a source of high-quality AAV. In our hands, the extent of GFP-OMM expression depends on the promoter construct used in the AAV, the viral titer and the pup's age[59], but tends to be more variable between experiments compared to a Cre-driver line crossing, option (i).

For both methods, we recommend comparing the Cre-dependent expression pattern in the MitoTag background with the described expression pattern from the literature (Steps 4–11), especially because even *Rosa26* knock-in mice can differ in their recombination efficiency when crossed to the same driver. Importantly, any off-target expression within the same tissue needs to be excluded (see asterisk in Extended Data Fig. 2c,e,f). Additionally, the established expression phenotype should be confirmed for the individual experimental setup (mouse age, tissue of interest, disease stage) and along the time course of experiments. For example, unused tissue material or adjacent tissues can be kept for this quality control, and immunostaining for cell-type markers and against GFP (i.e., to boost the GFP-OMM signal) can be performed for validation (Step 10B). Also, an increase or decrease in the yield of ICs from a given cell type over time is a sensitive indicator for a change in the expression profile. Hence, we recommend recording the IC yield as µg IC/mg tissue, the cell type, tissue, mouse sex and age per experiment.

Nongenetic, pathological conditions (such as high-fat diet or traumatic brain injury) can easily be introduced in [MitoTag/Cre] mice as with any other mouse line. By contrast, genetic perturbations related to disease phenotypes require advanced breeding schemes and validation of both the MitoTag and disease model. First, the introduction of disease alleles in combination with the MitoTag model (consisting of the MitoTag and *cre* alleles) requires a breeding strategy across multiple mouse generations, with substantial numbers of unsuitable animals, which in some jurisdictions can require specific legal consideration. Second, multiple breeding steps increase the risk of spurious recombination. To keep this risk low, we advise extra care when using already intercrossed [MitoTag/Cre] mice as breeders but, when possible, keeping the MitoTag and *cre* alleles separate until the experimental animal stage. Third, the genetic background of the various mouse lines might not be perfectly matched and compatible; so, the final genotype needs to be examined to ensure that neither the disease model's severity or time course, nor the MitoTag expression pattern have changed in an unexpected way.

Dominant disease models require (1) an intercrossing of the disease allele with the Cre-driver line (which then both are carried heterozygous) and (2) a homozygous MitoTag mouse colony. Mice from these two lines can then be intercrossed to yield 50% offspring that can be used as experimental animals: 25% MitoTag/Cre wild-type mice and 25% MitoTag/Cre mice that carry one copy of the dominant disease allele. To increase yield to 100% and if compatible with the disease allele, breeding an additional generation to obtain homozygous Cre drivers that also carry one copy of the disease allele, can be worth the extra time.

Recessive disease models (and most mutant mouse lines, in which studying cell-type-specific mitochondria is of interest) require first the generation of two breeding lines with the genetic outcome of: (1) homozygous MitoTag mice that carry one disease allele and (2) Cre-driver mice that are also heterozygous for the disease allele. These lines are then intercrossed to generate experimental animals at a frequency of 25% that all carry the MitoTag and the *cre* recombinase allele, of which half (12.5% of all offspring) lack the disease allele versus the other half that are homozygous disease allele carriers. If a heterozygous phenotype is of interest, 25% of offspring will carry that genotype together with the MitoTag/*cre* alleles. Again, if desired, the *cre* allele can be bred to homozygosity to double the yield, if no phenotype has been observed with homozygous Cre-driver mice.

As the *Rosa26* locus is localized on mouse chromosome 6, any disease model that requires a homozygous disease or mutant allele on chromosome 6 cannot be used together with the MitoTag mouse model (e.g., Atg7, a commonly deleted gene to block autophagy[67]). In this case, we advise using either a viral vector strategy introducing MitoTag expression in mice that carry two copies of the disease alleles, as well as Cre recombinase expression in the desired cell type, or a virus that expresses GFP-OMM directly under control of a cell-type-specific promoter. This viral vector could be directly injected into homozygous mice of the desired disease allele. We have so far only introduced Cre recombinase into MitoTag mice using AAVs, while Gella et al.[56] have successfully used an AAV-mitoTag virus with Tomm20-3XHA for a proteomics study on mitochondria from glutamatergic neurons. Further, such strategies have been reported for a viral RiboTag[68], suggesting this to be a possible extension of this protocol.

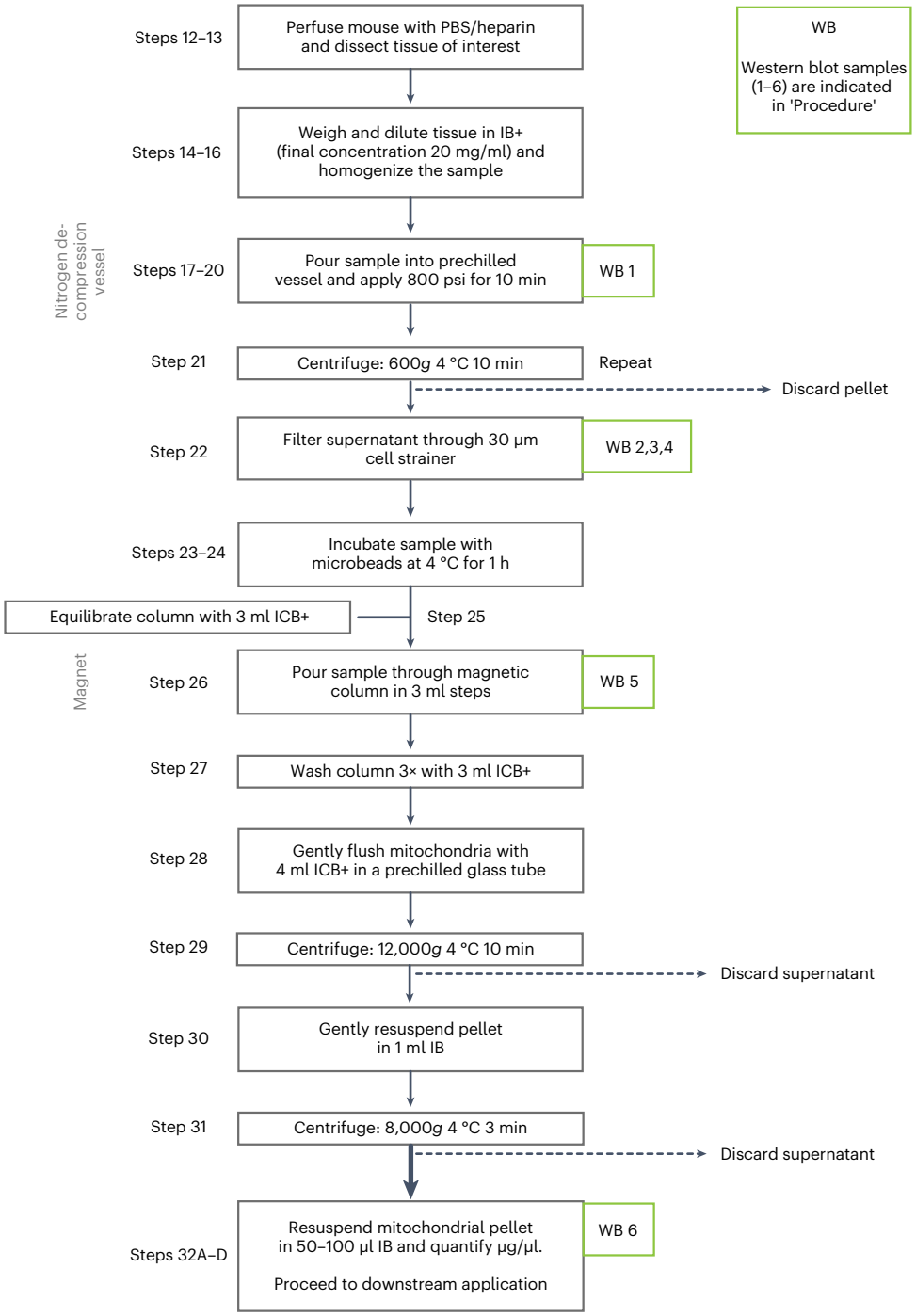

Fig. 2 | Outline of Steps 12–32 to capture cell-type-specific mitochondria. In Step 23, different types of microbeads can be used: for cell-type-specific mitochondria, anti-GFP microbeads and for bulk tissue mitochondria, anti-Tom22 microbeads. 1, whole cell lysate; 2, post-nuclear lysate; 3, cytosol; 4, crude mitochondrial fraction; 5, flow-through mito; 6, immunocapture (IC GFP or Tom). X+, buffer with BSA and protease inhibitor. For western blot recommendations, see Step 32B.

of GFP-OMM (Extended Data Fig. 1a). Upon presence of Cre recombinase, the stop sequence is excised from the genome, and Cre-expressing cells, as well as their lineage offspring, will express GFP-OMM. Thus, mitochondrial tagging is achieved by crossing MitoTag mice with suitable cell-type-specific Cre-driver lines. As the *Rosa26* locus supports expression in most cells[17], reporter expression is mostly driven by the past and present expression profile of the Cre-driver line. Alternatively, Cre-recombinase can be introduced via viral vectors. Hence, the MitoTag mouse model

Box 2 | Optimization of mitochondrial viability for functional assays

Several aspects of the IC are critical to keep mitochondria viable during the isolation and should be taken into consideration when adapting this protocol for other tissues. First, the buffer composition directly affects mitochondrial viability during the downstream analysis, and can be adapted according to the experimental design if needed. Importantly, when working with isolated mitochondria, the pH of buffers should be adjusted with K^+-based solutions at the temperature of intended use. Second, polysaccharide concentrations >20% during the IC (Step 23) impair antibody–antigen binding; hence, appropriate IB+ volumes for the tissue homogenate preparation should be calculated. Finally, the initial dilution of tissue in IB+ (Step 15) and the sample concentration during IC (Step 23) are critical factors for the viability of mitochondria. We illustrate this in Extended Data Fig. 4 for mitochondrial OCRs. Initial dilution around 20 mg tissue/ml IB+ results in a good mitochondrial respiration, while a lower dilution (5 mg tissue/ml) impacts the respiration of immunocaptured mitochondria (Extended Data Fig. 4b); thus, pooling of tissues may be necessary when working with a limited sample amount. Besides that, adjusting IC dilution concentrations, incubation time and amount of sample per column may increase the functionality of mitochondria post isolation, but also requires validation of cell-type-specific mitochondrial enrichment and purity (see 'spike-in' experiment, Fig. 4a–c). Importantly, Seahorse analysis was performed on isolated mitochondria with attached microbeads, which did not compromise the assay. A previous study[14] performed a comparison between IC Tom mitochondria and those isolated by differential centrifugation, concluding that bead-bound mitochondria after IC compare favorably with differentially centrifuged mitochondria.
To properly investigate the mitochondrial metabolic function, initial parameters need to be optimized via titration curves, most critically the amount of sample and CCCP concentration. The effective CCCP concentrantion will vary according to the amount and source of mitochondria, and needs to be determined for each substrate and tissue. Besides that, the CCCP concentration also depends on the amount of BSA in the MAS buffer, since BSA can directly chelate CCCP. Thus, buffers with higher BSA concentration require higher CCCP concentrations. For optimization of mitochondrial amount, the initial basal OCR should range from 20 to 160 pmol/min with respect to the cell type and substrate probed. Too little sample will result in very low basal OCR values, while too much sample will result in excessive oxygen consumption and ultimately, oxygen depletion. A non-linear drop in oxygen levels, as well as levels that do not fully recover before the next measurement, are signs of such oxygen depletion, which results in an artifactual response to compound injections. Thus, one needs to pay attention to the absolute oxygen tension, which should not drop below 20–50 mmHg at the end of the mesurement cycle. This parameter can be observed on the kinetic graph > Y1 > level within the Wave software.

represents a versatile tool to systemically investigate mitochondrial diversity in essentially any cell type for which a reliable Cre-driver line or viral gene delivery approach has been established.

Second, we optimized the IC protocol (Figs. 2 and 3) to obtain pure and functional mitochondria across different cell types and tissues. Importantly, the protocol minimizes any 'mixing events' between tagged and untagged mitochondria during the isolation process. This is critical, as mitochondria are dynamic organelles that share their content via constant cycles of fission and fusion. Such events occur inside cells but also ex vivo after organelle isolation[18]. To evaluate such organelle interactions, we used a 'spike-in' experiment (Fig. 4a), in which GFP-OMM expressing tissue is mixed with tissue from transgenic mice expressing mitochondrial matrix-localized red fluorescent protein (RFP; Thy1:mitoRFP[19]). This sample is then used for IC and analyzed for the presence of GFP-OMM and mitoRFP in the final sample via western blotting (Fig. 4b). In this setting, mitoRFP-labeled mitochondria represent a detectable population of organelles that should be de-enriched via IC GFP (Fig. 4c). We found that we were unable to separate GFP-OMM-tagged mitochondria from RFP-tagged organelles when using a standard protocol for mitochondrial isolation and beads ≥1 µm in diameter crosslinked with anti-GFP antibodies[20], despite obtaining intact and well-coupled mitochondria. This was presumably due to ex vivo fusion events enabled by organelle proximity on the surface of beads loaded with multiple mitochondria and further promoted by centrifugation. Therefore, key to minimizing these mixing events, while preserving mitochondrial viability, was (1) to keep tissue homogenates at a concentration of ~20 mg tissue/ml, (2) to avoid any mitochondrial pellet formation before IC, (3) to use antibody-coupled microbeads with a diameter of ~50 nm (Fig. 3c), and (4) to use an iso-osmotic KCl-based isolation buffer with ≤20% monosaccharide content.

We developed the MitoTag reporter mouse model and the related IC protocol primarily to define molecular and functional differences of mitochondria in cell types of the CNS[6], for instance, using proteomics to identify mitochondrial protein markers of neural cells or ex vivo assays to characterize differential bioenergetic or Ca^{2+} handling. When starting with the adult mouse cerebellum (~90 mg), we immunocaptured ~1.3 µg mitochondria per mg tissue from medium-abundant cell types, such as astrocytes (Fig. 5a). These amounts (typically >100 µg mitochondrial protein per cerebellum) are sufficient for standard mass spectrometry analysis, and we could quantify >3,000 proteins across 17 independent samples via label-free quantification[6]. Of those, >950 proteins are annotated as mitochondrial and of these >20% are differentially expressed among the three major neural cell types tested. Such a yield also allows for functional assays, e.g., mitochondrial bioenergetics or Ca^{2+} update assays. Thus, we expect that the MitoTag approach will be suitable for many other assays and cell types, without much optimization of this protocol. Still, when targeting small tissues (e.g., the retina) or rare cell types (e.g., interneuron subtypes), or aiming at parallel multiomics analyses from single samples, we advise that tissue pooling and protocol modifications be considered to maximize yield and sensitivity (Box 2).

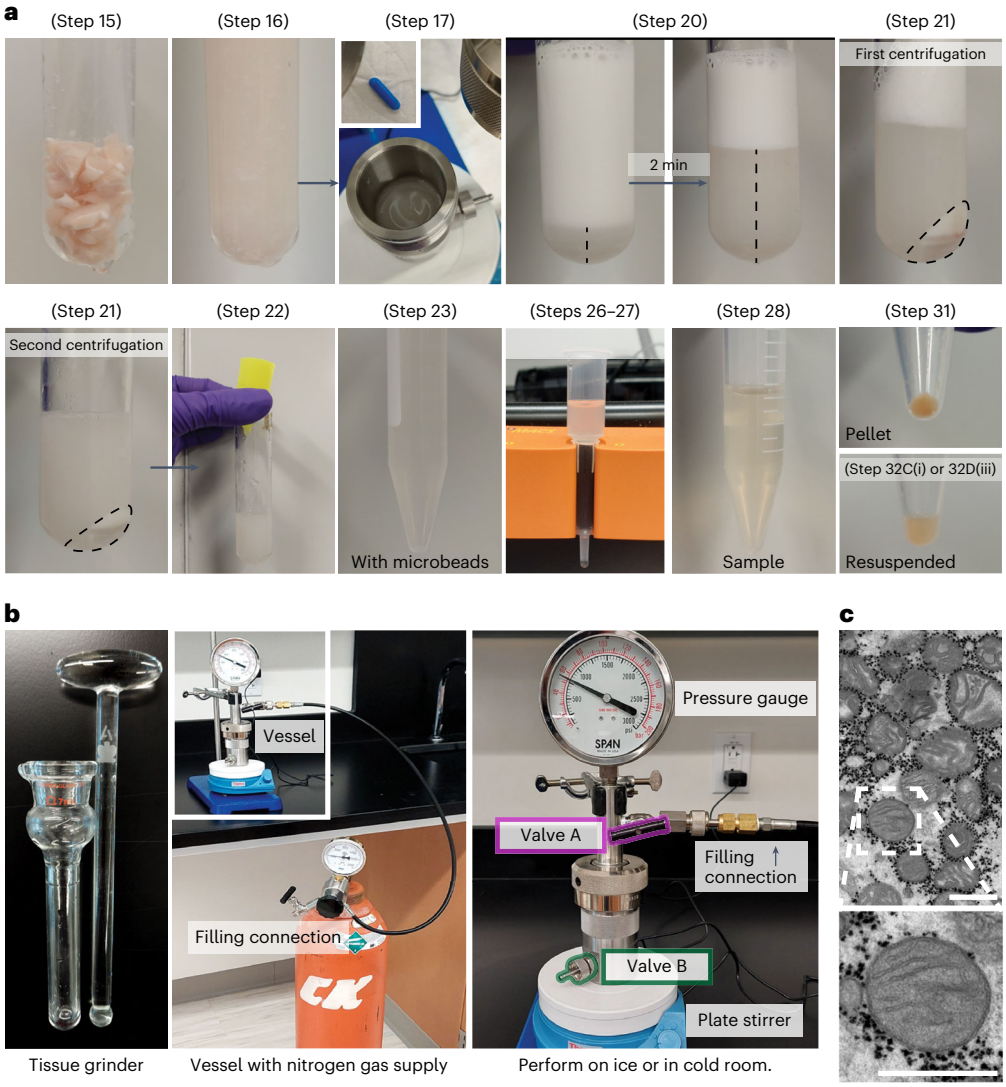

Fig. 3 | Sample pictures and tools for the capture of cell-type-specific mitochondria (Steps 15–32). a, Sample pictures illustrating the processing of tissue pieces towards the final sample of immunocaptured mitochondria. Step numbers relate to the 'Procedure' part of the article. Note, foam formation after cell disruption (Step 20) and the settling of foam within minutes (indicated by dashed line in Step 20, left versus right). Pellets after centrifugation steps have been circled with dashed lines. **b**, Tools for the homogenization of tissue (left) and the release of mitochondria from cells (middle, right). Left: a tissue grinder can be used for soft tissue in Step 15 (and should be size-matched to the studied tissue), while other tissues may require motor-driven grinders (Table 4 and Extended Data Fig. 3a). Middle: mitochondria are released from cells via nitrogen decompression. The disruption vessel is connected to a gas nitrogen supply. Right: in Step 17, the vessel is filled with sample, closed and connected to the nitrogen supply. Via valve A (magenta), the pressure inside the vessel is increased to 800 psi (Step 19). After 10 min, the sample is released through valve B (green) into a tube (Step 20). **c**, Electron micrograph of immunocaptured mitochondria. Microbeads are present as ~50 nm spots on the outer mitochondrial membrane. White dashed box is shown as detail below. Scale bars, 500 nm.

Applications of the method

The primary application of the MitoTag approach described here is to profile cell-type-specific mitochondrial populations that co-exist in the various cell types of a tissue; hence, allowing for the unmixing of the bulk mitochondrial tissue proteome, but also to characterize the specific functional adaptations of mitochondria in a given cell type. The approach allows—in contrast to inferring mitochondrial heterogeneity from transcriptomes or translatomes[21–23]—to characterize posttranslational protein modifications, as well as the effects of mitochondrial quality control and proteostasis. It provides information about the in situ phenotype of mitochondria, e.g., during development, dietary adjustments or aging. Furthermore, in the case of complex cellular geometries (as, e.g., of neurons), mitochondria from all cellular compartments can be isolated and characterized. Indeed, in the context of the CNS, the approach could be adapted to isolate mitochondria from specialized localizations (e.g., neuronal versus glial mitochondria from synaptosome preparations via IC Tom[24]) or neuronal

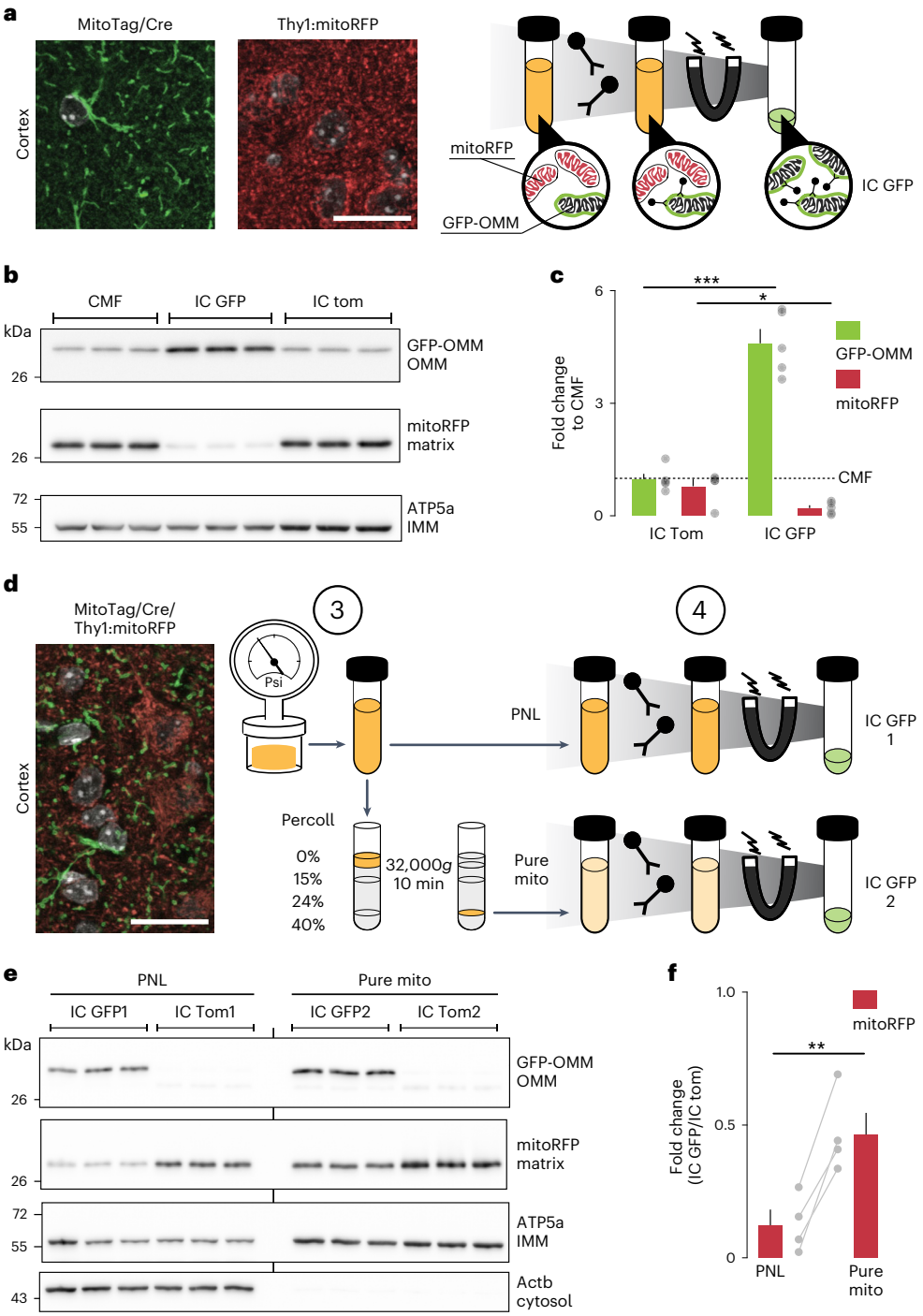

mitochondria from different cellular compartments of one neuronal subtype (e.g., surgically separated somato-dendritic versus axonal compartments of suitably chosen projection neurons; unpublished data by Marti Pastor, A., Guedes-Dias, P., Trovó, L. & Misgeld, T.). Finally, the MitoTag approach also enables the exploration of cell-type-specific mitochondrial changes in the context of disease models, as well as in sex-specific mitochondrial changes.

An obvious application for the method described here is the exploration of cell-type-specific mitochondrial adaptations that might explain the surprisingly specific manifestations of mutations in mitochondrial genes[25], and in the related quest to develop targeted mitochondrial therapeutic agents. For instance, in our previous work[6], we demonstrated that the most abundant excitatory neuron of the cerebellum, granule cells, prominently express the mitochondrial calcium uniporter (Mcu), while

◀ **Fig. 4 | Optimization and performance of the immunocapture protocol for cell-type-specific mitochondria. a**, Outline of 'spike-in' experiment to probe specificity of the IC protocol for GFP-OMM tagged mitochondria. For example, cortex from MitoTag/Emx1:Cre (green) is mixed with cortex from Thy1:mitoRFP (red) in a 1:1 weight ratio (left, confocal images from cortex). Here, mitoRFP mitochondria represent a detectable population of mitochondria that should be de-enriched in IC GFP. The mixed tissue lysate is enriched via anti-GFP microbeads resulting in a final sample of GFP-OMM tagged mitochondria (right). Nuclei are shown in gray. Scale bar, 20 µm. **b**, Western blot from 'spike-in' experiment outlined in **a**. Signal for GFP-OMM, mitoRFP and ATP5a, an endogenous mitochondrial protein, are shown. CMF from the initial tissue lysate (post-nuclear lysate, PNL); IC GFP, cell-type-specific mitochondria; IC Tom, bulk tissue mitochondria via anti-Tom22 microbeads. Submitochondrial localization: outer mitochondrial membrane (OMM), inner mitochondrial membrane (IMM) and mitochondrial matrix (matrix). Note, the GFP/RFP ratio is not altered between CMF and IC Tom, while an inverse relationship is observed for GFP/RFP in IC GFP. **c**, Quantification of 'spike-in' experiment described in **a**. Values are shown as fold change to the initial CMF from $N = 5$ isolations (GFP-OMM, green bars: $^{***}P = 0.0002$; mitoRFP, red bars: $^{*}P = 0.037$; one-tailed ratio-paired *t*-test). Densitometry is normalized to mitochondrial content. Bar graph: mean + s.e.m. with individual values. **d**, Outline of 'spike-in' experiment comparing the standard protocol (stage 3: input, PNL) to Percoll-purified mitochondria as input (pure mito). Here, cortex from MitoTag/Gfap:Cre/Thy1:mitoRFP mice was used as tissue source (for single-channel images, see Extended Data Fig. 5). From both input sources, mitochondria were immunocaptured via IC GFP as shown in figure and IC Tom (stage 4). Nuclei are shown in gray. Scale bar, 20 µm. **e**, Western blot from 'spike-in' experiment outlined in **d**. Signal for GFP-OMM, mitoRFP, ATP5a and the cytosolic protein Actb are shown for samples from the standard protocol (1) and the protocol with Percoll-purified mitochondria (2). Note, the absence of Actb and higher mitochondrial content (represented by ATP5a, mitoRFP and GFP-OMM) in Percoll-purified samples (pure mito). Localization: OMM, IMM, mitochondrial matrix (matrix) and cytosol. **f**, Quantification of mitoRFP signals in the experiment described in **d**. Values are shown as fold change IC GFP to IC Tom given that the input sources are vastly different in composition and purity. Bar graph: mean + s.e.m. with individual values from $N = 4$ independent experiments (mitoRFP, $^{**}P = 0.0027$, one-tailed paired *t*-test). Paired values are indicated by line. In **b** and **c**, All animal experiments were approved by the responsible regulatory agencies (Regierung von Oberbayern). Panels **b** and **c**, adapted from ref. [6], Springer Nature Ltd.

neighboring inhibitory neurons, Purkinje cells, have substantially lower levels (~30%) of this key regulator of mitochondrial Ca^{2+} levels. In mitochondrial Ca^{2+} uptake assays, this corresponds to an ~3-fold difference between these two adjacent neuronal cell types, and provides a surprising example of diversification of Ca^{2+} uptake[26] (Fig. 5c–e). Interestingly, Rmdn3, a novel mitochondrial marker protein that we identified for Purkinje cells, mediates endoplasmic reticulum–mitochondria contact sites—and indeed, we found mitochondria to be more tethered to the endoplasmic reticulum in Purkinje cells than in granule cells. Thus, the high expression levels of such a tether protein could explain how mitochondrial Ca^{2+} influx is maintained with low Mcu levels in Purkinje cells in vivo. This example illustrates how the MitoTag approach can be used for hypothesis generation based on comparing cell-type-specific mitochondrial proteomes, while immediately also providing the means to test such a hypothesis in ex vivo assays of mitochondrial function.

In this protocol, we focus on how the MitoTag approach can be applied to obtain functional characterization of cell-type-specific mitochondria using two common downstream assays, namely mitochondrial bioenergetics using the Seahorse analyzer and a plate-reader-based Ca^{2+} uptake assay. However, apart from these assays, a wide range of other approaches that are established for bulk tissue mitochondria, can be used to profile the phenotype of cell-type-specific mitochondria isolated by the here-described protocol. This includes measuring mitochondrial membrane potential, sequencing mitochondrial DNA mutations[27] or mitochondria-associated transcriptomes[28], profiling of post-translational protein modifications[29], complexome profiling[30], as well as metabolomics[16]. As biochemical and physiological properties of mitochondria are expected to differ between cell types, some assay optimization (e.g., for yield, purity and viability) will be required for each downstream application, just as they are commonly required for testing mitochondria from different tissues. For example, given that metabolites quickly exchange between compartments and are lost during long isolation processes, Bayraktar et al.[7] developed a MITO-Tag isolation workflow of ~10 min to investigate cell-type-specific mitochondrial metabolites from hepatocytes, which represent ~70% of the cells in the liver. Further optimization and validation of this metabolomics workflow will be needed to enable studies for medium-to-low-abundant cell types, e.g., from the CNS, as such a fast enrichment will probably not yield sufficient material. Ultimately, combined multiomics profiling of the global and local transcriptome, as well as the mitochondrial proteome and metabolome from individual cell-type-specific ICs would be a powerful—albeit challenging—application. Indeed, two organelle tag alleles (e.g. MitoTag and RiboTag) could be used in parallel[31], to isolate mitochondria and ribosomes from the very same cellular source in vivo. The genetics of such mouse crossings, the choice of suitable IC handles and the IC conditions that can reconcile the needs of the different omics measurements will require consideration that we are not covering here, even though we expect such applications to be possible.

A major area of anticipated application of this protocol is to explore mitochondrial phenotypes in mouse mutants and disease models. For example, in many neurodegenerative diseases, mitochondria are affected, and modeling of these diseases is challenging in vitro. Typically, little is known about the differential contribution of mitochondria to diseases across cell types (e.g., glial versus neuronal

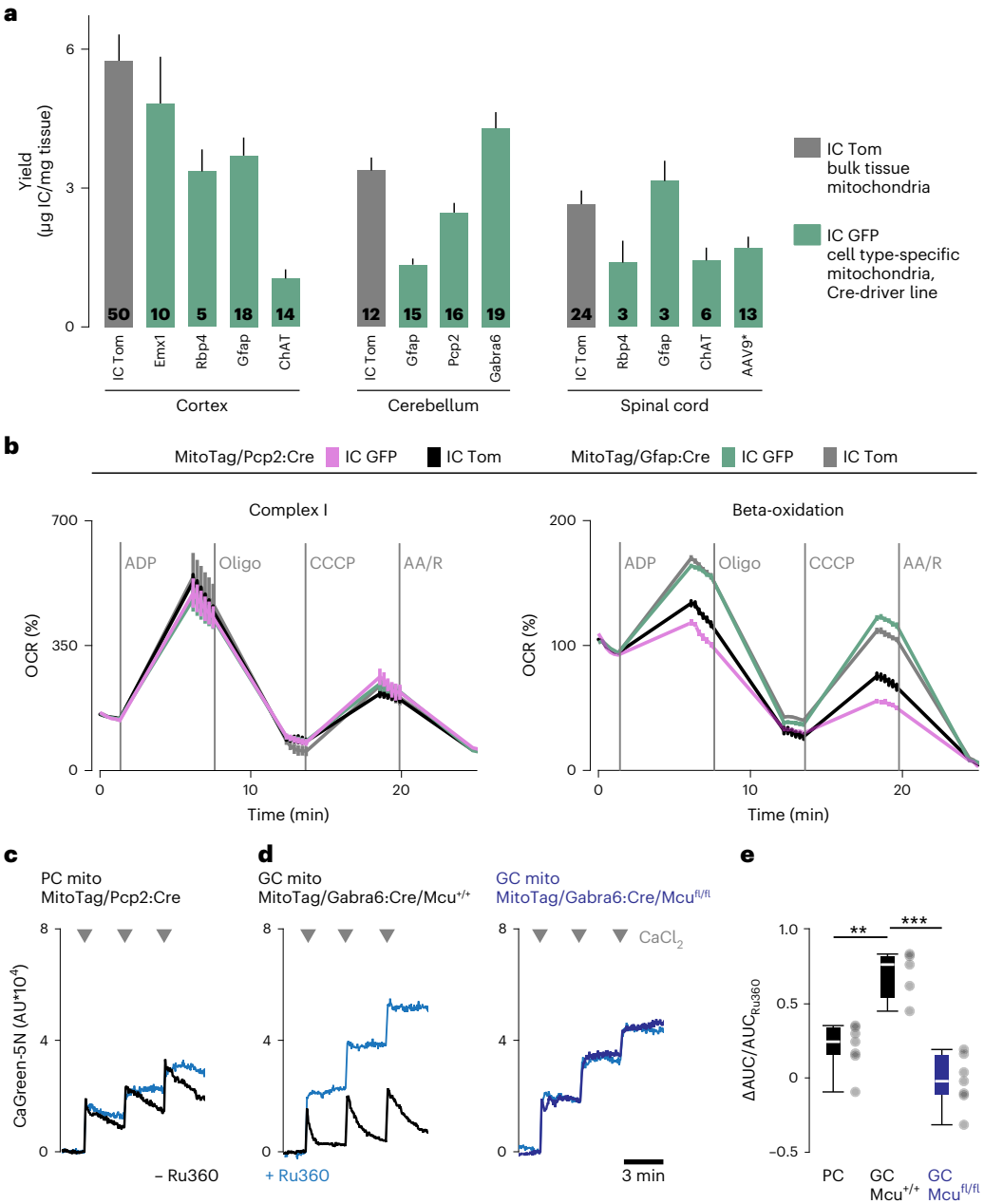

Fig. 5 | Anticipated results for IC and functional characterization of cell-type-specific mitochondria. a, IC yield (µg IC/mg tissue) from cortex, cerebellum and spinal cord using a variety of Cre-driver lines for GFP-OMM expression. IC Tom (gray), bulk tissue mitochondria via anti-Tom22 microbeads; IC GFP (green), cell-type-specific mitochondria. Bar graph: mean + s.e.m. Number of analyzed samples are indicated in bar graphs. **b**, Mitochondrial bioenergetics measured in immunocaptured mitochondria from cerebellum via the Seahorse analyzer. Mitochondria were isolated from Purkinje cells (magenta, MitoTag/Pcp2:Cre), cerebellar astrocytes (green, MitoTag/Gfap:Cre) and as bulk mitochondria from cerebellum (IC Tom, black/gray). Left: OCR via complex I (pyruvate/malate) from two experiments. OCR is shown as percentage of basal respiration with indicated injections. Line graph: mean ± s.e.m. from eight or more technical replicates. Right: OCR via beta-oxidation (L-palmitoylcarnitine/malate) from two experiments. OCR is shown as percentage of basal respiration with indicated injections. Line graph: mean ± s.e.m. from five or more technical replicates. Compounds are described further in Step 32D (xviii) and their injection is indicated with gray line: ADP, oligomycin A (Oligo), CCCP and antimycin A/rotenone (AA/R) for complex III and complex I inhibition, respectively. While cell-type-specific mitochondria from cerebellum show equal capacities to respire via complex I, the capacities are different utilizing beta-oxidation, as shown for Purkinje cell (magenta) and astrocytic (green) mitochondria. **c**–**e**, Ca^{2+} uptake assay performed in immunocaptured mitochondria from cerebellum via CaGreen-5N. Mitochondria were isolated from Purkinje cells (PC, MitoTag/Pcp2:Cre), granule cells (GC, MitoTag/Gabra6:Cre/$Mcu^{+/+}$) and from granule cells deficient in Mcu (MitoTag/Gabra6:Cre/$Mcu^{FL/FL}$). **c**, Line graph from one representative experiment probing PC mitochondria in the absence (black line) or presence of Ru360 (blue line, inhibitor of Mcu). Mitochondrial Ca^{2+} uptake is reflected by a decrease of extra-mitochondrial CaGreen-5N fluorescence after a 20 µM $CaCl_2$ pulse (gray triangles). **d**, Line graph from one representative experiment probing GC mitochondria from MitoTag/Gabra6:Cre/$Mcu^{+/+}$ cerebellum (black) and MitoTag/Gabra6:Cre/$Mcu^{FL/FL}$ cerebellum (dark blue) in the absence or presence of Ru360. **e**, Quantification of Ca^{2+} uptake at the first $CaCl_2$ pulse as $\Delta AUC/AUC_{Ru360}$ from $N \geq 5$ isolations. Box plot: median, quartile 1–3, whisker from minimum/maximum value, and individual data points (PC versus GC: $^{**}P = 0.0018$; GC $Mcu^{+/+}$ versus GC $Mcu^{FL/FL}$: $^{***}P < 0.0001$, one-way ANOVA with post hoc testing). **b** and **c**, adapted with permission from ref. [20]. All animal experiments were approved by the responsible regulatory agencies (Regierung von Oberbayern). Panel **b** adapted with permission from ref. [20]; **c**– **e**, adapted from ref. [6], Springer Nature Ltd.

mitochondria) given that bulk tissue mitochondria have so far been investigated. Certain pathological conditions (e.g., high-fat diet or traumatic brain injury) can easily be induced in [MitoTag/Cre] mice, while genetic disease models require advanced breeding schemes and further validation (Box 1).

Comparison with other methods

Traditionally, mitochondria are isolated by differential centrifugation[32–34] and can further be purified from other cellular components via density gradient centrifugation[35]. As an important step towards our approach, Franko et al.[14] introduced the isolation of mitochondria via immunoprecipitation using antibodies against the endogenous OMM protein Tom22. This approach yields mitochondria with a higher purity than obtained by differential centrifugation, yet they are less pure than those obtained via density gradient centrifugation. All three isolation methods produce bulk mitochondrial populations from animals, tissues or cultured cells, and much of our current knowledge of mitochondrial biology has been established through these techniques. Yet, in these bulk approaches, cell-type-specific mitochondrial phenotypes are masked, as the analysis is restricted to a heterogeneous population that comes from a typically uncharacterized mixture of cell types.

A practical alternative to characterize mitochondria of defined cell types would be cell culture models or cells acutely isolated from tissues by cell sorting, and subsequently isolate their mitochondria[36]. Alternatively, general proteomes of such cellular isolates can be generated and filtered through lists of known mitochondrial proteins[37]. Altogether, those approaches have substantial limitations: (1) they are restricted to a limited number of cell types, where suitable culture models or isolation protocols exist; (2) they are typically restricted to certain developmental stages; (3) they do not fully reflect the physiological state of mitochondria in vivo due to the metabolic effects of in vitro cultivation or ex vivo cell sorting; and (4) modeling of pathophysiological conditions is challenging in vitro, while for cell sorting, often only certain cell compartments can be isolated. Thus, the above mentioned techniques are not easily generalizable to many cell types and might not fully reflect mitochondrial diversity as it exists in vivo. The emergence of bioorthogonal labeling techniques to obtain cell-type-specific whole cell proteomes in situ[38,39], combined with increasingly complete mitochondrial protein compendia[37,40], might in the future provide a viable alternative that also delivers a cell-type-specific proteomic 'background', in which mitochondria are integrated. However, the current coverage of mitochondrial proteins in these published cell-type-specific proteomes remains low[38,39], and the fact that the MitoTag approach delivers not only a mitochondrial protein list but also the actual, functional organelle will remain a lasting advantage of the protocol presented here.

A direct approach to tackle cell-type-specific mitochondrial diversity could be to identify intrinsic biophysical or molecular differences between mitochondria from different cells in order to isolate them. To our knowledge, so far such approaches do not exist, simply due to lack of prior knowledge of suitable features of mitochondrial diversity across cell types. Notably, subcompartments of cells that contain mitochondria and have specific density features, allow isolation of mitochondrial subpopulations (e.g., synaptosomes[24]). Recently, Benador et al.[41] reported on the comparison of free mitochondria versus peri-droplet mitochondria from brown adipose tissue, which separate during differential centrifugation due to their attachment to lipid droplets. This unique setting provides important insights into the intracellular diversity of mitochondria that are currently largely unexplored; yet, they do not provide a solution for the systematic exploration of intercellular mitochondrial diversity. Furthermore, a number of reporter mice[42–44] exist that allow the expression of fluorescent proteins targeted to the mitochondrial matrix in specific cell types, making a FACS approach from crude mitochondrial isolates also conceivable[45]. Indeed, single mitochondrial approaches might be required for more specific studies, e.g., for studies of mitochondrial heterogeneity regarding physiology or genetics[46,47]. Still, this approach is restricted by the low yield and slow speed of mitochondrial FACS, even though special hardware adaptations can circumvent these limitations[45,48].

Notably, similar MitoTag approaches in animals were contemporaneously developed by other laboratories[7,16,27]. The first genetic in vivo model to investigate cell-type-specific mitochondria was published by Ahier et al.[27], who described a *Caenorhabditis elegans* model expressing the outer mitochondrial membrane tag Tom20-mKate2-HA under the control of a cell-type-specific promoter. Mitochondria from these worms were isolated with anti-HA paramagnetic beads and purity was assayed via a genetic mitochondrial DNA deletion model. Owing to the small size of nematodes, functional mitochondrial assays were performed on the population level requiring ~70,000 animals for one bioenergetic measurement. Despite this limitation, different patterns of genomic mitochondrial DNA alterations could be followed in individual cell types.

Furthermore, in parallel to the MitoTag mouse published by Fecher et al.[6], a similar mouse line, named MITO-Tag (JAX cat. no. 032290 at The Jackson Laboratory), was described primarily for the fast isolation of organelles and metabolomics[7]. This reporter mouse is also a *Rosa26* knock-in model with a Cre-dependent OMM tag. In the MITO-Tag mouse, the tag consists of 3XHA-GFP-OMP25, with the IC protocol targeting the HA-tag. Indeed, the protocols of Bayraktar et al.[7] and Fecher et al.[6] differ considerably in that they were optimized for different goals. The former was developed for a rapid (~10 min) isolation of mitochondria to perform metabolomics from an abundant cell type, while the protocol described here is geared for the selective and functional isolation of mitochondria from a defined, medium-to-low-abundant cell type in a heterogeneous tissue, such as the brain. Accordingly, the protocols differ in their details, most notably the type and size of beads used for magnetic separation (1 μm in ref. [7] versus 50 nm in ref. [6]). Still, while the protocol presented here has been tested and optimized for the MitoTag mouse[6], mitochondria from the MITO-Tag mouse[7] can—from our experience—also be isolated using the here described IC protocol with anti-GFP microbeads. Overall, both reporter mouse models appear interchangeable as tools with minor modifications, while the specific isolation process needs to be geared toward the downstream application.

Level of expertise needed to implement the protocol

In our experience, a technician, graduate student or postdoctoral researcher trained in standard molecular and biochemical techniques and with basic skills in microscopy and immunohistochemistry can perform Steps 4 to 32B–D of this protocol, from validation of the desired expression pattern, to tissue dissection, mitochondrial IC and downstream assays. However, establishing the MitoTag mouse colony and setting up suitable breeding with Cre-driver lines (Steps 1–3) and other genetic models requires substantial knowledge in mouse genetics and handling, as well as animal welfare regulations. Therefore, we recommend seeking advice from local core facilities or collaborators. Similarly, core facilities typically perform 'omics' analyses (Step 32A), and might have specific requirements for sample preparation that require outside expertise for implementation as part of a modified protocol. Finally, the downstream assays can be run in any laboratory that has access to the required specialized instrumentation (e.g., the Seahorse analyzer or related equipment) and can provide hands-on training in its use.

Limitations

While the presented protocol in our hands generates reproducible and robust results, e.g., in terms of mitochondrial yield and assay performance for established and validated [MitoTag/Cre] crossings, we would like to point out a few caveats and limitations for consideration before starting a MitoTag project.

The first and obvious limitation of the MitoTag approach is the fact that it requires a reporter mouse that expresses an artificial handle on the outer mitochondrial membrane. On the one hand, this necessitates complex and costly breeding schemes, but on the other hand, it also raises the specter of overexpression artifacts. While we controlled carefully for any spurious effects of this overexpressed neo-epitope on mitochondrial shape and dynamics in neurons[6], such possible artifacts need to be considered in any new application, and key results need to be confirmed by suitable methods on wild-type tissue.

Further, our protocol critically depends on the availability of suitable Cre-driver lines that faithfully induce the desired cell-type-specific expression of GFP-OMM. While such mice seem abundant in the literature, their intercrossing with different reporters and genetic drift can differ from the expected expression profile[49]—so finding a reliable and specific Cre-driver line for a given cell type can be a limitation.

Another limitation of this method—but this is shared with essentially any mitochondrial isolation method—is the need to adjust the protocol before applying it to new tissues and cell types. In any new setting, the needs for sufficient tissue homogenization or mitochondrial release from cells, as well as the composition of non-mitochondrial background proteins, might differ and adversely affect the efficacy or specificity of the MitoTag method. Thus, in any new setting, an initial revalidation of the IC performance is advised. Variables to consider are the tissue lysate concentration, the relative amount of microbeads used and the incubation time needed for labeling with microbeads (Steps 23–24). For instance, for small tissues, the lysate concentration should be within the range of 10–20 mg/ml and the pooling of material from multiple animals might be needed. For low-abundance cell types within larger tissues, we advise carefully validating the IC to achieve sufficient yield and viability for downstream assays (Box 2). Once the right parameters have been found, a 'spike-in' experiment with differentially labeled mitochondria can confirm the cell-type specificity of the modified protocol (Fig. 4a–c).

Researchers who want to use the MitoTag approach also need to consider the required level of purity of the mitochondria for their desired application. Mitochondria isolated via IC are purer than crude mitochondria isolated by differential centrifugation; however, they still contain more contamination from cytosolic proteins and adjacent organelles than isolated mitochondria from density gradient centrifugation[6,14]. Further purification of mitochondria via a Percoll gradient could improve purity, which should be considered if purity is a key parameter for downstream analysis. However, performing such steps before IC is problematic as mitochondria are forced into close proximity and fusion events can occur. Indeed, when we combined density gradient purification with IC, we could not achieve a comparable cell-type specificity as observed with the current protocol in 'spike-in' experiments (Fig. 4d–f). Hence, further purification steps that involve centrifugation should be limited to the final cell-type-specific IC with the caveat of lower yield and viability after density gradient centrifugation. Notably, in some contexts, contaminations are not necessarily detrimental, as they can carry biological information (e.g., about organelle contacts). We previously described the detection of peroxisomal proteins in our proteomes from astrocytic mitochondria as a possible functional engagement of the two organelles in fatty acid oxidation[6]. This metabolic pathway is shared between peroxisomes and mitochondria[50,51]. Hence, whether increasing the purity of immunocaptured mitochondria is necessary or even desirable depends on the biological question and the envisaged downstream applications.

Another set of potential limitations of the MitoTag approach relates to the ability to compare across tissues, time points or altered tissue states. In our previous work, we used a normalization strategy over bulk tissue mitochondria (IC Tom) to correct technical and biological variability among proteomes from different cell types. This experimental design works well when comparing mitochondria from multiple cell types within one tissue at one condition. However, when comparing across tissues (e.g., astrocytic mitochondria in cortex and cerebellum), this approach becomes more difficult, as the cell type abundance varies, but also non-mitochondrial contamination levels, mitochondrial mass and background proteomes substantially differ even between adjacent brain regions[2,52,53]. Similar limitations influence the comparison between developmental or disease states, or between mutant and wild-type animals—in essence any setting, in which the background proteome shifts. Several strategies to deal with this limitation can be considered. First, to reduce variability in comparisons between two tissues of the same animal, a direct pairwise comparison of measurements of tagged mitochondria from the same animal is advisable. Second, a core set of mitochondrial proteins can be defined[54,55], against which protein abundance is normalized, or the total mitochondrial peptide mass can be used for normalization. Finally, if two different tissues are compared and suitable material of matched control mice (i.e., non-MitoTag-expressing mice) is available, a crossover design can be used, where in one sample untagged tissue of one origin is 'mixed in' with tissue of another origin that contains tagged mitochondria and vice versa. This will balance the bulk proteome, to which the beads are exposed during IC, albeit at the cost of reducing the fraction of labeled mitochondria further, while also requiring more animals.

Finally, and most fundamentally, especially in disease-related applications, there remains the question of whether results obtained in MitoTag mice can be transferred to humans. We have observed that many of the cell-type-specific mitochondrial 'markers' that we identified in mouse, are conserved across species[20], including humans[6]. Hence, regarding mitochondrial density and shape, the approach already provided new tools to study cell-type-specific changes in human post mortem and biopsy tissue. Potentially, if conserved OMM proteins are identified as cell-type-specific markers, for which efficient antibodies exist or can be developed, such 'markers' could be used as endogenous IC handles (e.g., for the isolation of cell-type-specific mitochondria from human biopsies).

Experimental design

Considerations for the design of a MitoTag experiment can be grouped into two categories concerning (1) the genetic strategy to ensure proper MitoTag expression and allow combination, e.g., with disease alleles, and (2) the IC strategy tailored for specific tissues and cell types, while also accommodating the required yield, purity and expected variability for downstream assays.

Genetic strategy to ensure proper MitoTag expression

As described in Box 1, MitoTag expression is genetically prevented by the *loxP*-flanked stop cassette between the CAG promoter and GFP-OMM, and induced by the excision of this stop cassette by an otherwise expressed Cre recombinase. This genomic event is terminal and inherited by all daughter cells; hence, early developmental recombination can lead to substantial off-target cell expression of GFP-OMM, with the most extreme case being complete and inheritable recombination that includes

Table 1 | Summary of observed expression profiles in astrocytic MitoTag/Cre+ mice (related images are shown in Extended Data Fig. 2)

Cre-driver line	Panel in Extended Data Fig. 2	MGI	Cre expression	Observed expression or tissue
Tg(GFAP-cre)77.6Mvs/2J	2a	MGI:3838840	Astrocytes	All astrocytes; no issue
Tg(GFAP-cre/ERT2)505Fmv/J	2b	MGI:4458023	Astrocytes with TAM	Sparse recombination
Tg(Aldh1l1-cre)JD1884Htz/J	2c	MGI:5514359	Astrocytes	Leaky; germ line transmission
Tg(Sept4-cre)OX54Gsat/Mmucd	2d	MGI:5519914	Bergmann glia	All astrocytes
Tg(Plp1-cre/ERT)3Pop/J	2e	MGI:3695909	Oligodendrocytes with TAM[a]	Leaky; sparse astrocyte recombination
AAV9-CamKII 0.4.Cre.SV40	2f	/ UPenn: 105558-AAV9	Excitatory neurons	Sparse astrocyte recombination (transduction of neural progenitors at postnatal day 1–3)

[a]TAM, tamoxifen treatment at ≥2 weeks pf age.

the germline. While many Cre-diver lines are reliable in known settings, in new circumstances, unexpected recombination events are not uncommon[49]. Our protocol has been optimized using brain tissue derived from MitoTag crossings using well-established Cre-driver lines, which we further characterized for faithful specificity and efficacy[6]. Even in this setting, unexpected recombination occurred on several occasions (Table 1 and Extended Data Fig. 2). Thus, any MitoTag project using new Cre-driver lines or tissues should start by establishing the specificity of MitoTag expression in the tested cell type of interest (Box 1 and Steps 4–11). This evaluation needs to be continued throughout the project to avoid genetic drift and germline recombination, which is reported for many Cre-driver lines and arises from Cre-recombinase expression in oocytes and sperm[49]. Whole-animal recombination may be excluded during initial genotyping using primers that amplify a product between promoter and GFP-OMM. Similarly, induction via viral vectors should be evaluated for new viral batches and throughout larger projects with multiple injection cohorts. Regular checks of GFP-OMM expression are key, but we would even recommend fixing unused tissue from experimental animals to perform post hoc expression confirmation. Other indicators of altered expression patterns are an increase or decrease in IC yield for established cell types (Fig. 5a). This parameter can be monitored by recording the tissue weight, amount of lysate applied per separation column, column number and final yield (µg IC/mg tissue lysate). Any change in yield is an indicator for altered recombination, if all other parameters, such as lysate amount, microbead amount and incubation time, are kept constant.

The possibility of spurious recombination should be especially considered, when additional alleles, e.g., to model genetic disorders, are introduced (Box 1). The breeding scheme here should avoid recombined [MitoTag/Cre] mice as breeder mice, because germline recombination is more likely in this setting. Furthermore, any mouse model that requires two alleles (e.g., a homozygous knock-out) with localization on mouse chromosome 6, cannot be used with the MitoTag approach because the *Rosa26* locus, which harbors the MitoTag allele, is located on this chromosome. For this scenario, the use of a viral vector that either carries the MitoTag construct under control of a cell-type-specific promoter or delivers a tag under Cre recombinase control[56], could be considered. However, we have so far only transduced MitoTag mice with Cre-containing viruses[6].

Our protocol has been applied to a population of both male and female reporter mice (*Mus musculus*-C57BL/6 (mixed N/J) background) within an age range of 6 weeks to 6 months. Here, the sex of the mice did not affect the success of the protocol, and we believe that investigating cell-type-specific mitochondrial changes in a sex-dependent manner represents a meaningful future direction in certain disease contexts (e.g., metabolic syndrome). Finally, while this protocol can be applied to a wide variety of conditions, it is important to bear in mind that age and disease spectrum can substantially affect mitochondrial yield and functionality—as one would expect in the presence of primary or secondary mitochondrial pathology.

IC strategy

For the IC, we advise performing two isolations per experimental condition: one IC for GFP (IC GFP) and another for bulk tissue mitochondria using anti-Tom22 microbeads (IC Tom). While the first isolation represents the mitochondrial population of interest, the second isolation serves for the

correction of technical and biological variability across mice. For example, if two cell types within one tissue are examined in an assay, two mouse cohorts with different Cre-driver lines are necessary. These will have offspring at different time points, making it difficult to perform the IC and downstream assays at the same experimental run. Via the bulk tissue IC, the variability between such experiments can be estimated and normalized. Even if the same cell type is compared across two different tissues or tissue states, it is useful to obtain an IC Tom sample in addition to the cell-type-specific IC GFP mitochondria, given that these results can be compared with previously published data from bulk mitochondrial isolations and, e.g., to detect differences in mitochondrial mass or tissue-specific contaminations. To keep the IC as similar as possible between both conditions, paramagnetic microbeads with anti-GFP antibodies and anti-Tom22 antibodies from the same company can be used. We have successfully used this experimental design to identify mitochondrial diversity on the proteomic and functional level[6]. In contrast to other methods[7,16], we have not observed a benefit of including a control IC from wild-type cells or tissue (i.e., using anti-GFP microbeads on tissue from non-recombined MitoTag littermates). Such isolations do not yield mitochondria and, hence predictably, no signal in functional assays. While such controls may serve as unspecific background controls in proteomics and metabolomics studies, we have found in our study that most identified, non-mitochondrial proteins can be associated to interactions on the OMM of captured mitochondria. Therefore, these 'contaminations' would not be present in a control IC from wild-type tissue. If these non-mitochondrial proteins associate with captured mitochondria randomly, then their appearance is canceled out by the correction with bulk tissue mitochondria; if they are cell type specific, they should be considered and, at least in principle, could represent biologically meaningful interactions.

Materials

Biological materials

- MitoTag mouse line (Gt(ROSA)26Sor$^{tm1(CAG-EGFP*)Thm}$) generated as described above, available at the Jackson Laboratory (JAX no. 032675; MGI: 6296801; RRID: IMSR_JAX:032675)
- The Cre-driver mouse lines are listed in the following table:

Cre-driver line	MGI	Distributor, resource	Research resource identifiers
Emx1:Cre	MGI:2684610	Jackson Laboratory	RRID: IMSR_JAX:005628
Rbp4:Cre	MGI:4367068	UCD	RRID: MMRRC_031125-UCD
Gfap:Cre	MGI:3838840	Jackson Laboratory	RRID: IMSR_JAX:024098
ChAT:Cre	MGI:3699161	Jackson Laboratory	RRID: IMSR_JAX:006410
Pcp2:Cre	MGI:2174502	Jackson Laboratory	RRID: IMSR_JAX:004146
Gabra6:Cre	MGI:2450934	Ref. [57]	RRID: MMRRC_000196-UCD

! CAUTION Any experiments involving live mice must conform to relevant institutional and national regulations. All animal experiments were approved by the responsible regulatory agencies (Regierung von Oberbayern). **▲ CRITICAL** Animals used in this protocol were housed in a facility designed and operated in accordance with EU directive 2010/63 and the corresponding German animal welfare act and respective regulations. A maximum of five adult mice were housed in individually ventilated cage systems (Tecniplast) with food (Ssniff) and water ad libitum (refreshed weekly). To protect the animals from contamination, the cage systems were operated with overpressure and all cage changes were carried out under sterile bench conditions. Animals were kept in a 12 h light–dark cycle including twilight phases, and cages were enriched with retreat caves made of red plastic, paper towels, pressed cotton material ('nestlets') and small wooden sticks for nibbling.

Reagents

▲ CRITICAL This protocol was optimized to be used with the anti-Tom22 and anti-GFP microbeads, alongside the MACS Technology, from Miltenyi Biotec. The use of other beads or suppliers may alter the outcomes of the protocol due to the size of the beads, column incompatibility and possible interference of the bead with downstream assay, if still tagged to the mitochondria.

- Adeno-associated virus (AAV; UPenn Vector Core via Addgene; www.addgene.org/viral-service/penn-vector-core/) **! CAUTION** Use caution when handling AAV particles and follow the supplier's instructions and local regulations for personal protective equipment, handling and disposal.
- Genotyping primers (Integrated DNA Technologies):

Allele	Forward primer	Reverse primer
GFP-OMM	CAAGATCCGCCACAACATCG	TATCTCACGAAGGCCCAAAC
Rosa26 WT locus	GCACTTGCTCTCCCAAAGTC	CATAGTCTAACTCGCGACACTG
Cre recombinase	GGCAGTAAAAACTATCCAGC	TCCGGTATTGAAACTCCAGC

- Proteinase K (Biozym, cat no. 351100902)
- GoTaq(R) G2 Hot Start Green Master Mix (GoTag; Promega, cat. no. M7423)
- Nuclease-free water (New England BioLabs, cat. no. B1500S)
- Agarose (Seakem, cat. no. 50004)
- TAE 50× (Roth, cat. no. CL86.1)
- GelRed Nucleic Acid Gel stain (Biotium, cat. no. 41003) **! CAUTION** Wear personal protective equipment. Reagent intercalates with DNA and hence could be toxic.
- 1 kb plus DNA ladder (New England Biolabs, cat. no. N0469S)
- Ammonium sulfate (Sigma-Aldrich, cat. no. A4418)
- Gelatin (Sigma-Aldrich, cat. no. 48723)
- Sodium azide (Sigma-Aldrich, cat. no. S8032) **! CAUTION** Reagent is acutely toxic and should be handled under a fume hood and with personal protective equipment. Be extra careful as the reagent generates toxic gases upon mixing with water and acids.
- Tris-base (Sigma-Aldrich, cat. no. T1503)
- Fish gelatin (Sigma-Aldrich, cat. no. G7765)
- Fetal bovine serum (FBS, Sigma-Aldrich, cat. no. 10100147)
- Triton X-100 (Sigma-Aldrich, cat. no. T9284) **! CAUTION** Reagent is hazardous. Use personal protective equipment and avoid skin and eye contact.
- β-Mercaptoethanol (Sigma-Aldrich, cat. no. M6250) **! CAUTION** Reagent is hazardous. Use personal protective equipment.
- Paraformaldehyde (PFA; Sigma-Aldrich, cat. no. 158127) **! CAUTION** Reagent can be toxic upon inhalation, ingestion or skin contact. Handle under a fume hood and use personal protective equipment.
- Hoechst 33342 (Molecular Probes, cat. no. H3570) **! CAUTION** Reagent intercalates with DNA and is solved in dimethyl sulfoxide (DMSO). Use personal protective equipment when handling.
- Fluoromount-G mounting Medium (Thermo Fisher, cat. no. 00495802)
- Phosphate-buffered saline (PBS) 1× (VWR, cat. no. LONZ17-516F)
- PBS 10× (Thermo Fisher, cat. no. 70011044)
- Ultrapure water (Thermo Fisher, cat. no. 310977015)
- Distilled water
- Isofluran CP (CP-Pharma, cat. no. 1214) **! CAUTION** Reagent can be toxic upon inhalation or ingestion and irritating upon skin contact. Handle under a fume hood and use personal protective equipment.
- Heparin (Sigma-Aldrich, cat. no. H5512-25KU)
- Potassium hydroxide tablets (KOH, Merck, cat. no. 1.05033)
- D-Mannitol (Sigma-Aldrich, cat. no. M4125-1KG)
- D-Sucrose (Carl Roth, cat. no. 4621.1)
- HEPES (Carl Roth cat. no. 9105.3,)
- Disodium ethylenediaminetetraacetate dihydrate (EDTA, Sigma-Aldrich, cat. no. E5134)
- Ethylene glycol-bis(2-aminoethylether)-*N,N,N',N'*-tetraacetic acid (EGTA, Sigma-Aldrich, cat. no. E3889)
- Potassium chloride (KCl; VWR, cat. no. 1.04936.1000)
- Magnesium chloride ($MgCl_2$; Carl Roth, cat. no. KK36.1)
- Potassium dihydrogen phosphate (KH_2PO_4; Merck, cat. no. 104873)
- Fatty acid-free (FAF) BSA (Sigma-Aldrich, cat. no. A7030)
- cOmplete EDTA-Free Protease Inhibitor Cocktail (Sigma-Aldrich, cat. no. 5056489001)
- Anti-Tom22 microbeads, mouse (Miltenyi Biotec cat. no. 130-127-693)
- Anti-GFP microbeads, mouse (Miltenyi Biotec cat. no. 130-091-125)
- Pierce BCA Protein Assay kit (Thermo Fisher cat. no. 23225)
- Antibodies: anti-Actin (Sigma-Aldrich, cat. no. A2228, RRID: AB_476697), anti-Lamin B1 (Abcam,

cat. no. ab16048, RRID: AB_443298), anti-VDAC1/Porin (Abcam, cat. no. ab14734, RRID: AB_443084), anti-GFP (Santa Cruz Biotechnology, cat. no. sc-9996, RRID: AB_627695), anti-Tomm20 (Abcam, cat. no. ab78547, RRID: AB_2043078), anti-ATP5a (Abcam, cat. no. ab14748, RRID: AB_301447), anti-CypD (Abcam, cat. no. ab110324, RRID: AB_10864110), goat anti-mouse IgG (H + L)-HRP conjugate (Bio-Rad, cat. no. 170-6516, RRID: AB_11125547), goat anti-rabbit IgG (H + L)-HRP conjugate (Bio-Rad, cat. no. 172-1019, RRID: AB_11125143), chicken, anti-GFP antibody (Abcam, cat. no. ab13970, RRID: AB_300798), goat anti-mouse Fab fragments (Jackson ImmunoResearch Labs, cat. no. 115-007-003, RRID: AB_2338476), goat anti-chicken Alexa Fluor 488 (Thermo Fisher Scientific, cat. no. A-11039, RRID: AB_2534096)

- XFe96 FluxPak (XFe96 sensor cartridge, XF96 Cell Culture Microplates, Seahorse XF Calibrant Solution) (Agilent, cat. no. 102416-100)
- Succinic acid (Sigma-Aldrich, cat. no. S7501)
- L-Malic acid (Sigma-Aldrich, cat. no. M1000)
- L-Palmitoylcarnitine (Sigma-Aldrich, cat. no. 61251)
- Oligomycin A (Sigma-Aldrich, cat. no. 75351-5MG) **! CAUTION** Toxic product. Handle with care and use personal protective equipment.
- Adenosine 5′-diphosphate sodium salt (ADP, Sigma-Aldrich, cat. no. A5285)
- Carbonyl cyanide 3-chlorophenylhydrazine (CCCP, Sigma-Aldrich, cat. no. C2759) **! CAUTION** Toxic product. Handle with care and use personal protective equipment.
- Rotenone (Sigma-Aldrich, cat. no. R8875) **! CAUTION** Toxic product. Handle with care and use personal protective equipment.
- Antimycin A (Sigma-Aldrich, cat. no. A8674-25MG) **! CAUTION** Toxic product. Handle with care and use personal protective equipment.
- L-Glutamine (Sigma-Aldrich, cat. no. G3126)
- Calcium chloride, dihydrate ($CaCl_2$; CalBiochem, cat. no. 208290)
- CalciumGreen-5N (Thermo Fisher Scientific, cat. no. C3737)
- Ru360 (Sigma-Aldrich, cat. no. 557440) **! CAUTION** Toxic product. Handle with care and use personal protective equipment.
- Tri-sodium citrate (Roth, cat. no. 4088.3)
- Tween-20 (Sigma-Aldrich, cat. no. P1379)

Equipment

- PCR tubes, 0.2 ml (VWR, 781320)
- 24-Well plate (Cellstar cell culture plate, Greiner Bio-One, cat. no. 662160)
- Microscopy slides (Roth, cat. no. H870)
- Marienfeld Superior Precision Cover Glass, Thickness no. 1.5H (tol. ±5 µm), 24 × 50 mm, Electron Microscopy Sciences, cat. no. 71861-054)
- Sterile vacuum filter units with a pore size of 0.22 µm (Qpore, cat. no. QPPESBF250022)
- Nitrogen gas cylinder (Linde)
- 50 ml polypropylene Falcon tubes (Sarstedt, cat. no. 62.547.254)
- 15 ml polypropylene Falcon tubes (Sarstedt, cat. no. 62.554.002)
- Microcentrifuge tubes, 1.5 ml (VWR, cat. no. SARS72.706)
- Pre-separation filters (30 µm) (Miltenyi Biotec, cat. no. 130-041-407)
- LS columns (Miltenyi Biotec, cat. no. 130-042-401)
- 96-Well microplate, black, clear bottom, TC-Treated (Corning, cat. no. 353219)
- Vibratome (Leica, cat. no. VT1200)
- Confocal microscope (Olympus, e.g. model FV1000)
- Water bath (Haake)
- Fridge
- −20 °C freezer
- Dissection tools (Fine Science Tools)
- Peristaltic pump
- Analytical scale (Kern)
- Rotor homogenizer (Miccra)
- Dounce glass tissue homogenizer/A-pestle (Sigma-Aldrich, cat. no. D9063)
- Dounce tissue grinder glass tube with pestle (Kimble Kontes, size 20, cat. no. 886000-0020; size 22, cat. no. 886000-0022; size 23, cat. no. 886000-0023; size 24, cat. no. 886000-0024)

- Glass rod (Fisher Scientific, cat. no. S63447)
- Magnetic stirrer bar 7 × 2 mm (Fisher Scientific, cat. no. 10044234)
- Horizontal shaker (NeoLab)
- pH meter (Mettler Toledo)
- Centrifuges (Eppendorf, cat. no. 5424R; Beckman, cat. no. J2-MI)
- Centrifuge rotor (Beckman, cat. no. JA-25.50)
- Plate stirrer (NeoLab)
- Ice Pan, mini (Corning, cat. no. CLS432119-1EA)
- Cell disruption vessel 45 ml (Parr Instrument Company, model no. 4639)
- QuadroMACS Separator (Miltenyi Biotec, cat. no. 130-090-976)
- High-strength round-bottom glass tubes, 30 ml (Kimple, cat. no. 45500-30)
- Rubber adapter sleeves for 30 ml tubes (Kimple, cat. no. 45550-30)
- Multichannel pipette (Eppendorf)
- Non-CO_2 incubator (VWR)
- XFe96 Extracellular Flux Analyzer (Seahorse Bioscience, Agilent)
- Microplate reader (CLARIOstar; BMG Labtech)
- Thermomixer comfort (Eppendorf)
- PCR cycler (Eppendorf)
- PowerPac Basic Power Supply (BioRad, cat. no. 1645050)
- UV detection table with camera (VWR)

Software

- Microsoft Excel
- XFe96 Analyzer software
- Agilent Seahorse Wave desktop software

Reagent setup

! CAUTION Mitochondrial modulators, such as oligomycin A, rotenone and antimycin A, are toxic and should be handled with gloves. **▲ CRITICAL** Temperature alters the pH; thus, it is essential to pH the solutions at the specified temperature.

1 M HEPES–KOH pH 7.2

Dissolve 23.83 g HEPES in 80 ml of distilled water and adjust the pH to 7.2 with 5 M KOH at 37 °C. Adjust volume to 100 ml with distilled water and filter sterilize the solution. Store at room temperature (RT; 15–25 °C) for >6 months.

0.5 M EDTA–KOH

Dissolve 18.61 g of EDTA disodium salt hydrate in 80 ml of distilled water. Adjust pH to 7.4 using 5 M KOH and bring volume up to 100 ml with water. Store the solution at RT for several months.

5 M KOH

Dissolve 28.05 g in 100 ml distilled water. Store the solution at RT for several months.
! CAUTION Reagent is corrosive and toxic.

Isolation buffer (IB)

Add 220 mM mannitol, 80 mM sucrose, 10 mM HEPES and 1 mM EDTA, pH 7.4. Dissolve 10.02 g mannitol and 6.85 g sucrose in 200 ml distilled water. Add 2.5 ml of 1 M HEPES–KOH and 0.5 ml of 0.5 M EDTA–KOH to the solution, mix and cool to 4 °C in the fridge. Adjust the pH of the solution to 7.4 using 5 M KOH and adjust to a final volume of 250 ml. **▲ CRITICAL** The solution can be kept at 4 °C for 2–4 weeks. Before use, examine the solution for mold growth or precipitation.

Isolation buffer with 1% BSA and protease inhibitor (IB+)

For 100 ml IB+, dissolve 1 g of FAF-BSA in 100 ml IB. Add 1× protease inhibitor and store at 4 °C.
▲ CRITICAL The solution should be prepared on the day of the experiment and cannot be stored.

1 M KCl

Dissolve 37.28 g of KCl in 500 ml of distilled water and store the solution at RT for several months.

1 M $MgCl_2$
Dissolve 9.52 g of $MgCl_2$ in 100 ml distilled water. Store at RT for >6 months. ▲ **CRITICAL** Mg^{2+} can compete with Ca^{2+} in various settings and therefore it is essential to prepare it accurately. Using plastic instead of glassware for long-term storage reduces the level of free Ca^{2+} contamination, which is a critical parameter in the assay.

1 M KH_2PO_4
Dissolve 13.61 g of KH_2PO_4 in 80 ml of distilled water. Adjust the pH to 7.2 with KOH or HCl at 37 °C and complete the volume to 100 ml with distilled water before filter sterilizing the solution. Store at RT for several months.

IC buffer (ICB)
137 mM KCl, 2.5 mM $MgCl_2$, 3 mM KH_2PO_4, 10 mM HEPES and 1 mM EDTA, pH 7.4. Combine 34.25 ml of 1 M KCl, 0.625 ml of 1 M $MgCl_2$, 0.75 ml of 1 M KH_2PO_4, 2.5 ml of 1 M HEPES and 0.5 ml of 0.5 M EDTA in 210 ml distilled water. Cool to 4 °C before adjusting the pH to 7.4 with 5 M KOH. The solution can be kept at 4 °C for 2–4 weeks.

ICB with 1% BSA and protease inhibitor (ICB+)
For 100 ml ICB+, dissolve 1 g of FAF-BSA in 100 ml ICB. Add 1× protease inhibitor and store at 4 °C. ▲ **CRITICAL** The solution should be prepared on the day of the experiment and cannot be stored.

0.5 M EGTA–KOH pH 7.2
Dissolve 9.51 g of EGTA in 35 ml of distilled water and adjust the pH to 7.2 with KOH at 37 °C. Complete the volume to 50 ml with distilled water and store at RT for several months. ▲ **CRITICAL** EGTA poorly dissolves in water and the resulting solution is very acidic. Since a large amount of KOH is needed, we recommend to start dissolving KOH tablets until pH is ~7.0, and then continue with a 5 M KOH solution added dropwise. EGTA is an important modulator of Ca^{2+} concentration and therefore it is essential to prepare it accurately.

2× Mitochondrial assay buffer (MAS)
140 mM sucrose, 440 mM mannitol, 20 mM KH_2PO_4, 10 mM $MgCl_2$, 4 mM HEPES and 2 mM EGTA, pH 7.2. Dissolve 23.96 g of sucrose, 40.07 g of mannitol and 2 g of essentially FAF-BSA in 350 ml of distilled water. Add 10 ml of 1 M KH_2PO_4, 5 ml of 1 M $MgCl_2$, 2 ml of 1 M HEPES–KOH and 2 ml of 0.5 M EGTA–KOH. Adjust the pH to 7.2 at 37 °C with KOH. Adjust the volume to 500 ml with distilled water and filter sterilize the solution. Store at 4 °C for up to 3 months.

1× MAS with substrates (60 ml)
Add the respiratory substrates to 30 ml of 2× MAS according to Table 2, and supplement with 0.2% FAF–BSA. Complete the volume with distilled water to 60 ml and keep the solution at RT until further use.

2 M NaOH
Dissolve 8 g of NaOH in 100 ml distilled water. Store the solution at RT for several months **! CAUTION** Reagent is corrosive and toxic.

400 mM ADP
Dissolve 4 g of ADP in 15 ml of distilled water and heat up to 37 °C. Adjust the pH to 7.2 at this temperature with KOH or HCl and adjust the volume to 20 ml. Prepare 500 µl aliquots and store at −20 °C for >6 months.

2.5 mM oligomycin A
Equilibrate vial to RT and dissolve 5 mg of oligomycin A in 2.53 ml of DMSO. Prepare 20 µl aliquots and store at −20 °C for several months. **! CAUTION** Toxic product. Handle with care and use personal protective equipment.

Table 2 | Amounts of mitochondria (µg/well) needed per substrate and tissue (Step 32C(xii))

Substrates	Complex I, 10 mM pyruvate, 2 mM malate		Complex II, 10 mM succinate, 2 µM rotenone		Beta-oxidation, 50 µM L-palmitoylcarnitine, 2 mM malate	
	µg mitos	µM CCCP	µg mitos	µM CCCP	µg mitos	µM CCCP
Cortex	2	10	1	10	nd	nd
Cerebellum	3	7.5	2	7.5	8	3
Spinal cord	3.5	10	2.5	10	nd	nd

nd, not determined.

100 mM and 10 mM CCCP
Equilibrate the 100 mg CCCP to RT before opening the vial. Dissolve the powder in 4.89 ml of DMSO to obtain the 100 mM stock solution. Mix 400 µl of 100 mM CCCP with 3.6 ml of DMSO to obtain a 10 mM solution. Prepare aliquots of 35 µl and store at −20 °C for several months.

25 mM palmitoyl-L-carnitine
Dissolve 50 mg of palmitoyl-L-carnitine in 5 ml of distilled water. Prepare aliquots of 25 µl and store at −20 °C for several months.

500 mM and 2.5 mM rotenone
Equilibrate vial to RT and dissolve 1 g of rotenone in 5.1 ml of DMSO. This generates a 500 mM stock solution. Prepare aliquots of 0.5 ml. Dilute 20 µl of 500 mM rotenone in 3.98 ml of DMSO to obtain a 2.5 mM stock solution. Prepare aliquots of 30 µl and store at −20 °C for several months. **! CAUTION** Toxic product. Handle with care and use personal protective equipment.

10 mM antimycin A
Equilibrate vial to RT and dissolve 25 mg of antimycin A in 4.56 ml of DMSO. Prepare 20 µl aliquots and store at −20 °C for several months. **! CAUTION** Toxic product. Handle with care and use personal protective equipment.

0.5 M succinate
Dissolve 2.95 g of succinic acid in 40 ml of distilled water. Adjust pH to 7.4 with KOH at RT and adjust volume of succinate solution to 50 ml with distilled water. Prepare 0.5 ml aliquots and store at −20 °C for several months. Do not freeze and thaw.

0.5 M malate
Dissolve 3.35 g of L-malic acid in 40 ml of distilled water. Adjust pH to 7.4 with KOH at RT and adjust volume to 50 ml with water. Prepare 0.5 ml aliquots and store at −20 °C for several months. Do not freeze and thaw.

0.5 M glutamate
Dissolve 3.68 g of L-glutamic acid in 40 ml of distilled water. Adjust pH to 7.4 with KOH at RT and adjust volume to 50 ml with water. Prepare 0.5 ml aliquots and store at −20 °C for several months. Do not freeze and thaw.

0.5 M pyruvate
Dissolve 1.1 g of pyruvic acid in 15 ml of distilled water. Adjust the pH to 7.2 at 37 °C using KOH or HCl. Adjust volume of pyruvate solution to 20 ml with distilled water and store as 0.5 ml aliquots at −20 °C for >6 months. Avoid freeze–thaw cycles.

Respiration buffer (RB)
137 mM KCl, 2.5 mM $MgCl_2$, 3 mM KH_2PO_4 and 10 mM HEPES, pH 7.4. Combine 13.7 ml of 1 M KCl, 0.25 ml of 1 M $MgCl_2$, 0.3 ml of 1 M KH_2PO_4 and 1 ml of 1 M HEPES in 100 ml ultrapure water. Adjust pH to 7.4 with KOH and adjust volume of RB to 100 ml with distilled water. The solution can be stored at 4 °C for 2–4 weeks. Before use, bring solution to RT.

RB with supplement (RB+)
100 nM Calcium Green-5N, 5 mM succinate, 5 mM malate, 5 mM glutamate and 0.2% BSA. For 10 ml RB+, add 2.38 µl of Calcium Green-5N stock, 0.1 ml of 0.5M succinate, 0.1 ml of 0.5 M malate, 0.1 ml of 0.5 M glutamate and 0.02 g of FAF-BSA to 9.7 ml RB. Prepare this solution fresh for each experiment.

420 µM Calcium Green-5N stock solution
Bring reagent to RT and dissolve 0.5 mg in 1 ml ultrapure water. Prepare 15 µl aliquots and store it at −20 °C protected from light for >6 months. Avoid freeze–thaw cycles.

1 M $CaCl_2$
Dissolve 14.701 g of calcium chloride dihydrate in 100 ml ultrapure water. Store at RT for several months.

1 mM Ru360 stock solution
Dissolve 0.5 mg of Ru360 in 909 µl ultrapure water, make 15 µl aliquots and store them at −20 °C for >6 months. Do not freeze–thaw aliquots. **! CAUTION** Toxic product. Handle with care and use personal protective equipment.

Gitocher buffer pH 8.8 10×
670 mM Tris-base, 166 mM ammonium sulfate, 65 mM magnesium chloride and 0.1% gelatin, pH 8.8. Dissolve 8.12 g of Tris-base, 2.19 g of ammonium sulfate and 1.32 g of magnesium chloride in 90 ml ultrapure water. Adjust pH to 8.8 with HCl and add 0.1 g of gelatin. Adjust volume of Gitocher buffer to 100 ml with distilled water and store indefinitely at RT.

10% Triton X-100
Combine 10 ml Triton X-100 with 90 ml ultrapure water. Mix overnight on a horizontal shaker and store indefinitely at RT. **! CAUTION** Reagent is hazardous. Use personal protective equipment and avoid skin and eye contact.

Proteinase K extraction buffer
Add 1× Gitocher buffer, 0.5% Triton X-100, 1% β-mercaptoethanol and 0.5 µg/ml proteinase K, pH 8.8. For 2 ml buffer, combine 0.2 ml of 10× Gitocher buffer with 0.1 ml of 10% Triton X-100 and 20 µl of β-mercaptoethanol in 1.68 ml of ultrapure water. Add 1 µg of proteinase K to a final concentration of 0.5 µg/ml. **▲ CRITICAL** The buffer needs to be prepared fresh and cannot be stored.

4% PFA/PBS pH 7.4
Solve 4g of PFA in 80 ml distilled water by heating the solution on a plate stirrer at 300 rpm at 50 °C. Add two drops of 2 M NaOH to the solution and wait until dissolved. Remove the solution from the heating plate and cool to RT. Filter the solution through a paper filter and add 10 ml of 10× PBS pH 7.4. Adjust volume of PFA/PBS to 100 ml with distilled water and test pH with pH paper. Adjust pH with HCl or NaOH, if need and use within 24 h or aliquot and freeze at −20 °C for >6 months.

0.8% sodium azide/PBS pH 7.4
Dissolve 0.8 g of sodium azide in 90 ml distilled water under a fume hood. Add 10 ml of 10× PBS pH 7.4 and store indefinitely at 4 °C. **! CAUTION** Reagent is acutely toxic and should be handled under a fume hood and with personal protective equipment. Be extra careful as the reagent generates toxic gases upon mixing with water and acids.

1× PBS/heparin solution pH 7.4
Dissolve 25 KU of heparin in distilled water to make a stock concentration of 19.5 U/ml. This solution can be stored at 4 °C for >6 months. Before the experiment, dilute heparin stock by adding 130 µl to 50 ml 1× PBS pH 7.4.

Blocking solution
2% BSA, 2% fish gelatin and 2% FBS in 1× PBS pH 7.4. Dissolve 2 g of FAF-BSA and 2 g of cold fish gelatin in 80 ml distilled water. Add 2 ml of FBS, 10 ml of 10× PBS pH 7.4. Adjust volume of blocking solution to 100 ml with distilled water. Aliquot the solution and store it at −20 °C for up to 1 year.

Heat-mediated antigen retrieval solutions

Sodium citrate buffer pH 6.0

10 mM Tri-sodium citrate and 0.05% Tween-20. Dissolve 0.147 g of tri-sodium citrate and 0.25 ml of 10% Tween-20 in 40 ml ultrapure water. Adjust the pH to 6.0 with NaOH and adjust buffer volume to 50 ml with distilled water. Solution can be store at 4 °C for up to 6 months.

EDTA buffer pH 8.0

1 mM EDTA and 0.05% Tween-20. Dissolve 0.019 g of EDTA and 0.25 ml of 10% Tween-20 in 40 ml ultrapure water. If EDTA does not dissolve, add a drop of NaOH. Adjust the pH to 8.0 with HCl or NaOH and adjust buffer volume to 50 ml with distilled water. Solution can be store at 4 °C for up to 6 months.

Tris-EDTA buffer pH 9.0

10 mM Tris-base, 1 mM EDTA and 0.05% Tween-20. Dissolve 0.06 g of Tris-base, 0.019 g of EDTA and 0.25 ml of 10% Tween-20 in 40 ml ultrapure water. Adjust the pH to 9.0 with HCl and adjust buffer volume to 50 ml with distilled water. Solution can be store at 4 °C for up to 6 months.

Tris buffer pH 10.0

10 mM Tris-base and 0.05% Tween-20. Dissolve 0.06 g of Tris-base and 0.25 ml of 10% Tween-20 in 40 ml ultrapure water. Adjust the pH to 10.0 with NaOH or HCl and adjust buffer volume to 50 ml with distilled water. Solution can be stored at 4 °C for up to 6 months.

Procedure

Cell-type-specific expression of GFP-OMM using MitoTag reporter mice ● Timing 6–8 weeks (without mouse line import)

1 Import the homozygous MitoTag mouse line from the Jackson Laboratory (JAX, cat. no. 032675 (Rosa26–CAG–LSL–GFP–OMM)).

▲ **CRITICAL STEP** Consult with your animal care facility about the specific legal regulations, import requirements and procedures (time range 4 weeks to 4 months, depending on whether a rederivation is necessary).

2 Keep MitoTag mice as a pure homozygous line to maximize the output of experimental animals in later [MitoTag/Cre] crossings. Animals are viable and fertile without any reported phenotype. Animal housing conditions can be found under the 'Materials' section; however, the protocol should not be impacted by any other approved housing condition.

▲ **CRITICAL STEP** Animal breeding needs to adhere to the relevant regulations and guidelines for vertebrates and be approved by the local governmental institutions or equivalent.

3 Induce GFP-OMM expression in the cell type of interest. This can be achieved via option A, homozygous MitoTag mouse intercrossing with a Cre-driver line, or option B, viral delivery of Cre recombinase into heterozygous MitoTag neonates. As discussed in 'Experimental design', both strategies have important benefits and limitations, and the individual scientific question will determine which method is more appropriate or easier to establish.

(A) **Homozygous MitoTag mouse intercrossing with a Cre-driver line ● Timing 8 weeks (excluding mouse line import)**

(i) Import cell-type-specific Cre recombinase driver mouse lines (Cre-driver line) of choice. Useful resources are for instance: the Cre Portal at Jackson Laboratory (www.jax.org/research-and-faculty/resources/cre-repository/characterized-cre-lines-jax-cre-resource), MMRRC (www.mmrrc.org) and MGI webpage (www.informatics.jax.org). As this process is limited by local facility regulations, it may take 3–4 weeks for a mouse line import or up to 4 months if a rederivation is necessary.

(ii) Breed Cre-driver lines as instructed by the vendor or source and according to its reference.

▲ **CRITICAL STEP** Genetic drift can alter the expression pattern of Cre lines over time, particularly in transgenic lines with random genome insertions (Box 1). Moreover, germline or other spurious recombination events are more common than typically assumed, so that we recommend histological confirmation of GFP-OMM expression patterns for every experimental animal using a small sample from the tissue of interest or adjacent material not used for the experiment (for immunohistochemistry, see Steps 4–11). As most tissues cannot be extracted without killing the animal (or require an approved animal protocol with surgery), this step is performed while dissecting experimental material (Step 13).

(iii) To induce GFP-OMM expression, intercross MitoTag mice with the Cre-driver lines of choice. Each Cre-driver line crossing will create experimental mice for a specific cell type. Both sexes can be used for the MitoTag allele. The breeding schema, including the number of crossings necessary for the experimental design, should align with recommendations for the used Cre-driver line.

▲ **CRITICAL STEP** The number of necessary crossings is highly variable and depends on several factors: (1) the Cre line used—can a homozygous versus heterozygous mice be used for breeding?; (2) the abundance of the cell type of interest—do multiple mice need to be pooled to recovery a minimum amount of material, e.g., from dopaminergic neurons?; (3) the downstream protocol application. For example, a proteomic study requires four to six biological replicates per group, while a seahorse experiment might require five mice in total with different substrates investigated.

(iv) To genotype the offspring for both alleles (GFP-OMM and Cre) with allele-specific primers, collect tissue material from mice in 0.2 ml PCR tubes by either ear-punch or tail-tip biopsy.

▲ **CRITICAL STEP** Material collection needs to adhere to local animal welfare regulations and be approved by the responsible agencies.

? TROUBLESHOOTING

(v) Add 50 µl Proteinase K extraction buffer to an ear punch or 150 µl to a tail tip.

(vi) Incubate the reaction in a PCR cycler with the following program:

Step	Temperature	Time
1	55 °C	5 h
2	95 °C	5 min
3	4 °C	On hold

■ **PAUSE POINT** DNA samples can be stored at 4 °C for up to 6 months.

(vii) Centrifuge DNA samples at 16,000*g* at RT for 5 min.

(viii) To amplify PCR products for GFP-OMM and the *cre* allele with strain-specific PCR primers (Table 3), generate a Master Mix sufficient for the number of mice plus three controls: water control, positive control for the tested allele and negative control (wild-type DNA), as follows. Reactions for the Rosa26 WT and GFP-OMM allele can be performed in one tube, while the Cre recombinase allele should be performed separately.

Reagent	Amount for 1× reaction	
2× GoTaq Master Mix	10 µl	*X* (number of mice +3 controls)
Strain-specific PCR primers (10 pmol/µl; see Table 3):		
Forward primer	1 µl	
Reverse primer	1 µl	
Nuclease free water	Adjust to 19 µl	

Table 3 | Strain-specific PCR primers for genotyping (Step 3A(viii))

Allele	Primer	Sequence 5′–3′	T_m	Product size	Note
GFP-OMM	Forward	CAAGATCCGCCACAACATCG	58 °C	324 bp	Perform GFP-OMM and Rosa26 WT locus PCR in one tube
	Reverse	TATCTCACGAAGGCCCAAAC			
Rosa26 WT locus	Forward	GCACTTGCTCTCCCAAAGTC	58 °C	600 bp	
	Reverse	CATAGTCTAACTCGCGACACTG			
Cre recombinase[a]	Forward	GGCAGTAAAAACTATCCAGC	60 °C	650 bp	
	Reverse	TCCGGTATTGAAACTCCAGC			

[a]If available, Cre-driver line specific PCR primer should be used.

▲ **CRITICAL STEP** The three controls ensure proper evaluation of the PCR performance and should always be included for each genotyping experiment.

(ix) In 0.2 ml PCR strips, add 19 µl PCR Master Mix and 1 µl of DNA sample from Step 3A(vi). Vortex and amplify with the following PCR reaction cycle:

Cycle no.	Denaturing	Annealing	Extension	Hold
1	95 °C for 5 min			
2–33	95 °C for 15 s	T_m[a] for 30 s	72 °C for 15 s	
34			72 °C for 5 min	
35				4 °C

[a]T_m is set according to the primers used. See Table 3.

■ **PAUSE POINT** PCR products can be stored at 4 °C for up to 7 days or −20 °C for several weeks.

(x) Cast a 1.5% agarose gel in 1× TAE buffer with 1× GelRed Nucleic Acid Gel stain.
! CAUTION Wear personal protective equipment to avoid exposure to GelRed dye.

(xi) Load 10 µl of a 1 kb plus DNA ladder into the first lane followed by 10 µl of each PCR reaction per lane.

(xii) Run the gel at 100 V for 30 min or until the loading dye front has passed 70% of the gel length.

(xiii) Use a UV light detection instrument to visualize the PCR product bands (Extended Data Fig. 1b). Record image and dispose gel according to local regulations.
! CAUTION Wear personal protective equipment to avoid exposure to UV light.

(xiv) After genotyping, confirm cell-type-specific GFP-OMM expression for each [MitoTag/Cre] crossing in the tissue of interest (Steps 4–11).
▲ **CRITICAL STEP** Confirm the absence of GFP-OMM expression in off-target cell types within the same tissue for specificity.

? TROUBLESHOOTING

(B) **Viral delivery of Cre recombinase in heterozygous MitoTag neonates** ● **Timing 6–8 weeks**

▲ **CRITICAL** The approach described here is one of many viral strategies to deliver Cre recombinase to MitoTag mice. For other approaches and animal ages, consult ref. [58].

(i) Acquire AAV of suitable serotype with cell-type-specific promoter and Cre recombinase expression cassette, for example from the Penn Vector Core via Addgene (www.addgene.org/viral-service/penn-vector-core/).
▲ **CRITICAL STEP** When choosing an AAV for a cell type of interest, consider the appropriate serotype, titer and length of the cassette. The appropriate virus titer needs to be established for the cell type of interest and validated for each virus batch. High viral titer may transduce most target cells, however, at the risk of cytotoxicity.

(ii) Breed wild-type females with homozygous MitoTag males resulting in a litter of 100% heterozygous MitoTag offspring.
▲ **CRITICAL STEP** Note that genotyping is not needed for option 3B.

(iii) Upon birth, transfer both the litter and its mother to the experimental facility.
▲ **CRITICAL STEP** This minimizes environmental stress before viral injection.
▲ **CRITICAL STEP** The father remains in the breeding facility and can be used for future crossings.

(iv) Following the instructions in Wang et al.[59], to perform the intraventricular viral injection.

(v) Observe mice for 48 h followed by returning them to the animal facility.

(vi) At the experimental age of interest, confirm cell-type-specific GFP-OMM expression in AAV transduced MitoTag mice in the tissue of interest (Steps 4–11). Expression can be observed as early as 1 week postinjection; however, the expression pattern can change with age and hence, evaluation should be performed at the experimental age of choice.
▲ **CRITICAL STEP** Confirm the absence of GFP-OMM expression in off-target cell types within the same tissue for specificity.

? TROUBLESHOOTING

Validation of cell-type-specific GFP-OMM expression ● Timing 3–4 days

▲ CRITICAL GFP-OMM expression should be validated in combination with cell-type markers if available. Depending on the staining protocol, endogenous GFP fluorescence can be used or needs to be enhanced with antibodies, e.g., if antigen retrieval methods are used that eliminate native GFP fluorescence.

4 Kill animals with an approved method that does not impair transcardial perfusion. For example, place animal in 10 × 10 cm box with an isoflurane-soaked swab. The swab should not touch the animal's skin. Wait until the animal does not show respiratory movement of the thorax, has lost all reflexes and no heartbeat is palpable. Remove the animal from the box and continue with Step 5, in which the right atrium is cut. For the evaluation of a new [MitoTag/Cre] crossing, three to five animals from two or three litters should be examined.
▲ CRITICAL STEP The procedure requires approval from the local governmental institutions or equivalent.

5 Under a fume hood, pin down the animal on all limbs and open its thorax. Place the perfusion needle into the left ventricle tip and cut the right atrium while starting the perfusion at a speed of 2 ml/min using a peristaltic pump. Perfuse the animal with 5 ml 1× PBS/heparin solution.
▲ CRITICAL STEP PBS/heparin solution allows removing blood from organs, reducing autofluorescence from blood cells.

6 Change the solution to 4% PFA/PBS pH 7.4 and perfuse the animal for an additional 10–15 min.
▲ CRITICAL STEP Skeletal muscle contractions occur within 3 min of 4% PFA/PBS perfusion and indicate a good perfusion.

7 Dissect tissue of interest and submerge in fresh 4% PFA/PBS overnight at 4 °C.

8 Wash the tissue with 1× PBS under slow agitation and at RT for 10 min. Repeat this step twice.
■ PAUSE POINT Fixed tissue can be stored for up to 6 months without the loss of endogenous GFP-OMM fluorescence when submerged in 1× PBS/0.8% sodium azide at 4 °C and protected from light.

9 Cut 30–50 µm thick tissue sections using a vibratome.
■ PAUSE POINT Tissue sections can be stored in 1× PBS/0.8% sodium azide at 4 °C protected from light for up to 4 weeks.

10 To examine GFP-OMM expression by confocal microscopy either using native fluorescence or in combination with immunostaining, perform the following steps in a 24-well plate, on a horizontal shaker at 85 rpm at RT and protected from light, if not indicated otherwise. Use option A for endogenous GFP-OMM fluorescence and option B for GFP-OMM immunostaining (alone or with cell-type markers).

(A) **Endogenous GFP-OMM fluorescence**

(i) Immerse tissue section in 300 µl of 0.1% Triton X-100/PBS with nuclear stain (for example, Hoechst 33342) for 5 min.
! CAUTION Wear personal protective equipment to avoid exposure to stain.

(ii) Wash section with 1× PBS for 2 min. Repeat this step once.

(iii) Mount section straight onto a microscopy slide, remove excessive liquid, add a drop of Fluoromount Mounting Medium and top with a #1.5 cover glass. Fix the cover glass with nail polish and cure the mounting medium at 4 °C in the dark. Continue to Step 11.
■ PAUSE POINT Mounted sections can be stored for at least 1 month at 4 °C protected from light.

(B) **GFP-OMM immunostaining (alone or with cell-type markers)**

(i) Immerse tissue section in 300 µl of 0.5% Triton X-100/PBS and incubate for 30 min.
▲ CRITICAL STEP The permeabilization step should be independently optimized for the needed cell-type markers and can vary between antibodies. In certain cases, heat-mediated antigen retrieval is needed (Step 10B(iii–vii)).

(ii) Wash section with 1× PBS for 5 min. Repeat twice.

(iii) If no antigen retrieval is needed, skip to Step 10B(viii). If heat-mediated antigen retrieval is required, transfer tissue section to a 2 ml tube and add antigen retrieval buffer.

(iv) Heat water bath to 90 °C.

(v) Transfer sample tube to water bath and incubate for 30 min.

(vi) Cool sample down at 4 °C for 5 min.

(vii) Transfer tissue section to a 24-well plate and wash with 1× PBS for 5 min. Repeat twice.

(viii) Block tissue section with 200 µl of Blocking solution for 1 h.

(ix) Wash section with 1× PBS for 5 min.

(x) If a primary antibody produced in mouse is used, block tissue section with 1:100 anti-mouse Fab fragments in 1× PBS for 1 h.
▲ **CRITICAL STEP** Endogenous IgGs in the mouse tissue can cause a substantial amount of background when they are not blocked before antibody incubation. Alternatively, primary antibodies produced in mouse should be avoided.
(xi) Dilute primary antibodies in 10% Blocking solution/PBS.
(xii) Incubate section with antibody solution overnight at 4 °C under agitation.
■ **PAUSE POINT** Primary antibody incubation can be extended to up to 3 days, if kept at 4 °C.
(xiii) Wash section with 1× PBS for 10 min. Repeat twice.
(xiv) Dilute secondary antibodies in 10% Blocking solution/PBS.
! **CAUTION** Endogenous GFP-OMM fluorescence may be present (dependent on antigen retrieval, Step 10B(iii)); hence, a secondary antibody for the 488 nm channel should be chosen for the anti-GFP antibody.
(xv) Incubate section with secondary antibodies for 2 h.
(xvi) Wash section with 1× PBS for 10 min. Repeat twice.
(xvii) Immerse section in 1× PBS with nuclear stain (e.g., Hoechst 33342) for 5 min.
! **CAUTION** Wear personal protective equipment to avoid exposure to stain.
(xviii) Wash section with 1× PBS for 2 min. Repeat this step once.
(xix) Mount section straight onto a microscopy slide, remove excessive liquid, add a drop of Fluoromount Mounting Medium and top with a #1.5 cover glass. Fix the cover glass with nail polish and cure the mounting medium in the dark at 4 °C.
■ **PAUSE POINT** Mounted sections can be stored for at least one month at 4 °C and protected from light.

11 Image tissue section using a confocal microscope equipped with the required laser lines and filter sets to detect the used fluorophores. Given the small size of mitochondria, we recommend using a 40×/1.35 N.A. oil immersion objective or higher.

? TROUBLESHOOTING

Mouse killing, tissue homogenization and plasma membrane permeabilization

● **Timing 30 min per animal**

▲ **CRITICAL** We provide a protocol for isolating mitochondria from soft mouse tissues such as brain, liver and kidney. The isolation should be performed swiftly and will differ depended on the complexity of the experiment (e.g., dissection of tissue areas and pooling of animals). The number of animals required will depend on the cell-type-specific mitochondria of interest, the tissue and the downstream analysis to be performed, and can be estimated based on the mitochondrial yield (for more information, see 'Anticipated results').

▲ **CRITICAL** After tissue collection, all steps should be performed on ice or in a cold room. This preserves mitochondrial function and avoids structural damage caused by the activity of proteases and phospholipases.

12 Kill mice from Step 3 without impairing transcardial perfusion, as detailed in Steps 4–5.
▲ **CRITICAL STEP** The number of animals will depend on the downstream application and can vary from one to six or more animals. This is related to the cell-type abundance of interest and downstream assay requirements.
▲ **CRITICAL STEP** The procedure requires approval from the local governmental institutions or equivalent.
▲ **CRITICAL STEP** Complete Steps 12–15 for each animal before processing the next—except for the case where tissue from multiple animals is pooled. Here the tissue can be transferred to a tube with 1× PBS/heparin on ice and stored for up to 1 h.
▲ **CRITICAL STEP** Whole-body perfusion avoids the release of hemoglobin from blood cells when these are ruptured during the isolation. It also stops erythrocytes from sedimenting with mitochondria after taking up mannitol from the buffer, which would contaminate subsequent functional assays on isolated mitochondria.
▲ **CRITICAL STEP** The perfusion time should be kept consistent between animals and experiments.
? TROUBLESHOOTING

Table 4 | Summary of tissue grinders shown in Extended Data Fig. 3a with reference to volume, clearance and sample recommendation

No.	Volume	Clearance	Comment	Sample
A	7 ml	0.07–0.12 mm (pestle A) 0.02–0.06 mm (pestle B)	By-hand homogenization, 3 strokes Three strokes	Soft tissue (brain)
20	3 ml			Brain, subregions
22	8 ml	0.10–0.15 mm	By-hand or motorized at 300 rpm, five strokes	Brain, subregions
23	17 ml			Brain, subregions
24	45 ml			Liver

13 Dissect the tissue or region of interest and place it on a weigh boat on ice. If interested in isolating mitochondria from several tissues, collect the other tissues from the animal and store them on ice.
▲ **CRITICAL STEP** Collect suitable extra tissue from the same tissue or adjacent regions to monitor GFP-OMM expression in every experimental animal used (Steps 7–11). There should be enough material to obtain a few tissue sections after fixation (Step 9).

14 Weigh out the sample.

15 Place sample in a prechilled Dounce glass homogenizer of the proper size (Fig. 3a, Table 4 and Extended Data Fig. 3) on ice with the corresponding volume of IB+ to achieve the recommended concentration of 20 mg tissue/ml IB+.
▲ **CRITICAL STEP** Concentrations down to 10 mg tissue/ml do not affect the IC but can reduce the coupling of isolated mitochondria, as observed via mitochondrial bioenergetics (Extended Data Fig. 4).
▲ **CRITICAL STEP** A volume of less than 3 ml is difficult to process in the nitrogen decompression vessel (Step 17).
■ **PAUSE POINT** Samples can be kept in a tube with IB+ on ice for ~1 h before further processing.

16 Homogenize the tissue (Fig. 3a) with a pestle connected to a rotor-homogenizer at 300 rpm with five strokes. If not available, perform three up-and-down strokes with a glass Dounce homogenizer by hand (Fig. 3b, left). This step dislodges the tissue and creates a single-cell suspension. It improves tissue homogenization and avoids clogging valve B of the nitrogen decompression vessel (Fig. 3b, right, green valve).
? TROUBLESHOOTING

17 Confirm that valve B of the prechilled nitrogen decompression vessel (Fig. 3b, right, green valve) is tightly closed, and that the vessel is equipped with a magnetic stirrer bar (Fig. 3a and Supplementary Video 1). Transfer the homogenate into the vessel.
▲ **CRITICAL STEP** When working with volumes of homogenate smaller than 3 ml, it is necessary to place the sample in a small glass beaker that can be placed inside the vessel cylinder to avoid sample loss during recovery.

18 Keep temperature for plasma membrane permeabilization ≤4 °C by either placing the cell disruption vessel on ice or by performing the procedure in a cold room.

19 Close the vessel and attach the filling connection to a nitrogen gas supply as indicated in the instruction manual (Fig. 3b, middle). Check that all valves are closed including the release valve on the nitrogen gas supply. Pressurize the cell disruption vessel to 800 psi by slowly opening the nitrogen suppliers and then valve A on the decompression vessel (Fig. 3b, right, magenta valve). Wait ~30 s; if the pressure drops due to gas absorbance by the sample, readjust the pressure and incubate for 10 min. Depending on the sample volume used (3–35 ml), the incubation time can be adjusted (5–20 min).
▲ **CRITICAL STEP** A pressure of 800 psi selectively permeabilizes the plasma membrane of mammalian cells leaving the mitochondrial membrane and other organelles intact.
? TROUBLESHOOTING

20 Hold a prechilled 50 ml tube in front of the vessel valve B (Fig. 3b, right, green valve) and slowly depressurize the vessel by opening valve B. The sample will foam while exiting the vessel, which is a sign of cell permeabilization (Fig. 3a). For independent western blot analysis (Step 32B), collect a 100 µl aliquot of the sample, which represents the whole cell lysate (WCL), and store it at −20 °C until further use.
▲ **CRITICAL STEP** It is recommended to become familiar with the sample collection step before performing the experiment, as the sample might rapidly exit the decompression vessel and be lost during collection.

21 Centrifuge the whole cell sample at 600*g* at 4 °C for 10 min and transfer the supernatant to a new tube using a pipette without touching the pellet (Fig. 3a). Discard the pellet and repeat the centrifugation once.
▲ **CRITICAL STEP** To minimize contamination, avoid disturbing the pellet, which contains cell debris, intact cells and nuclei. Plasma membrane lipids can be observed as foam on top of the supernatant (Fig. 3a, picture for Step 21) and should not be carried over. For that, place the pipette in the middle phase (supernatant) when transferring the sample, or discard the lipid foam first.

22 Collect the supernatant with a pipette and pass it through a 30 µm cell strainer placed on top of a new tube on ice (Fig. 3a). This is the post-nuclear lysate (PNL). For independent western blot analysis (Step 32B), collect a 100 µl aliquot of PNL. Additionally, collect a 250 µl aliquot of PNL and centrifuge at 12,000*g* at 4 °C for 3 min. The resulting supernatant represents the cytosolic fraction (Cyto) and is transferred to a new tube. Wash the remaining pellet in IB+ without BSA and repeat the centrifugation once. Discard the supernatant from the washing step. The pellet represents the crude mitochondrial fraction (CMF). Store western blot samples at −20 °C until further use.

IC of cell-type-specific mitochondria ● Timing 90 min

23 Combine 1–2 ml of PNL from Step 22 with 9 ml ICB+ and 50 µl antibody-coated microbeads in a prechilled 15 ml tube on ice (Fig. 3a). For the capture of GFP-OMM tagged mitochondria, anti-GFP microbeads are used (IC GFP), while a bulk tissue mitochondrial isolation can be performed with anti-Tom22 microbeads (IC Tom).

24 Incubate the sample on a horizontal shaker at 60 rpm at 4 °C for 1 h.

25 Toward the end of the incubation period, place a LS column with its wings facing forward into a QuadroMACS Separator and equilibrate the column with 3 ml ICB+. Prepare one column per IC.

26 At the end of the incubation period, place the sample on ice and apply it onto the column in 3 ml steps (Fig. 3a). Let the solution run through the column via gravity. The microbead-labeled mitochondria are retained in the column due to the magnetic field, while unlabeled organelles, as well as any other cellular components run through the column as flow-through. For independent western blot analysis (Step 32B), collect the flow-through in a 30 ml high-strength glass tube and centrifuge at 12,000*g* at 4 °C for 10 min. Discard the supernatant and wash the pellet in IB twice. This is the untagged mitochondrial fraction (FT mito). Store western blot sample at −20 °C until further use. This sample allows estimating the IC performance and the enrichment over other cellular fractions to be estimated (Step 32B).
▲ **CRITICAL STEP** When using a 30 ml high-strength glass tube, always use the recommended rubber adapters.
? TROUBLESHOOTING

27 Wash the column with 3 ml ICB+. Wait until the column is empty to repeat this step twice. Discard all flow-through.

28 Remove the column from the QuadroMACS Separator, apply 4 ml ICB+ to the column reservoir and slowly flush the solution out into a prechilled tube using the supplied plunger. Multiple samples can be pooled in one 30 ml high-strength glass tube for centrifugation in the next step.
▲ **CRITICAL STEP** Apply constant and controlled pressure to the plunger and avoid collecting the foam at the end.

29 Centrifuge at 12,000*g*, 4 °C for 10 min.
▲ **CRITICAL STEP** When using 30 ml high-strength glass tubes, always use the recommended rubber adapters.

30 Discard the supernatant, place the mitochondrial pellet on ice and carefully dislodge it using a glass rod. Resuspend the pellet in 1 ml IB+ (without BSA), and transfer it to a tube on ice.
▲ **CRITICAL STEP** Use a cut pipette tip to resuspend the mitochondrial pellet to minimize shearing forces and avoid the formation of bubbles that could compromise the functionality of mitochondria. Immunocaptured mitochondria are associated with microbeads as shown by electron microscopy (Fig. 3c). In functional assays, no adverse effect has been reported for mitochondrial isolations with paramagnetic beads[14].
? TROUBLESHOOTING

31 Centrifuge at 8,000*g* at 4 °C for 3 min and discard the supernatant (Fig. 3a).

32 Cell-type-specific mitochondria are now ready to be used in downstream applications. While there are many mitochondrial assays described in the literature, we give instructions for the following common options: Use option A for proteomics analysis; option B for western blot analysis; and options C and D

for assays probing mitochondrial functions ex vivo: option C to analyze mitochondrial bioenergetics with the Seahorse analyzer, and option D to analyze mitochondrial calcium uptake.

(A) **Proteomics analysis**

(i) Resuspend the pellet in 1 ml IB without EDTA and protease inhibitor.

▲ **CRITICAL STEP** EDTA and protease inhibitor can interfere with sample preparation steps for mass spectrometry.

(ii) Centrifuge at 8,000*g* at 4 °C for 3 min and discard the supernatant. Repeat once.

(iii) Remove all solution from the pellet and flash freeze the sample in liquid nitrogen.

■ **PAUSE POINT** Sample can be stored at −80 °C indefinitely.

(iv) Continue with sample processing for mass spectrometry (for example, SP3 (see ref. [60])) or transfer samples to a core facility/collaborator.

▲ **CRITICAL STEP** Of note, paramagnetic beads can interfere with liquid chromatography–tandem mass spectrometry (LC–MS/MS) and damage mass spectrometry instruments. Care should be taken to eliminate these particles during sample preparation (e.g., via in-gel digest or centrifugation) or peptide desalting with C18 Stage tips before LC–MS/MS.

? TROUBLESHOOTING

(B) **Western blot analysis**

▲ **CRITICAL** Multiple samples have been collected for western blotting analysis throughout the 'Procedure'. These are: WCL (Step 20), PNL (Step 22), Cyto (Step 22), CMF (Step 22), mitochondria from IC flow-through, FT mito (Step 26), and ICs: IC GFP and IC Tom (Step 31). These samples can be used to validated cell type specificity and purity of immunocaptured mitochondria, i.e., from other untagged organelles and cellular components.

(i) Assess IC efficiency and sample purity using a standard western blot protocol (see ref. [6] for instructions).

(ii) For antibody recommendations, see Table 5.

(C) **Assays probing for mitochondrial functions: measurement of mitochondrial bioenergetics with the Seahorse analyzer ● Timing 90–120 min**

▲ **CRITICAL** For protocol outline, see Fig. 6.

(i) One day before the experiment, hydrate the XFe cartridge with 200 µl of water. Place cartridge and 30 ml of Agilent Seahorse XF Calibrant in a non-CO_2 incubator at 37 °C overnight.

(ii) Before starting the mitochondria isolation, remove the XFe cartridge from the incubator and replace the water with 200 µl of the Agilent Seahorse XF Calibrant using a multichannel pipette.

(iii) Cool the XFe96 Cell Culture Microplate on ice and start the tissue processing (Steps 12–22) and IC of mitochondria (Steps 23–31)

(iv) Gently resuspend the pellet from Step 31 in a small amount of IB on ice (Fig. 3a).

▲ **CRITICAL STEP** Immunocaptured mitochondria should be used for functional assays within 1–2 h for best performance.

(v) Quantify the protein concentration of samples by BCA protein assay or other protein quantification methods (e.g., 660 nm Protein Assay). Test several dilution factors of the sample (25×, 50× and 100×) in triplicates to obtain an accurate sample concentration.

▲ **CRITICAL STEP** For reproducible results, ensure to use the same quantification method for all samples and the same standard for the calibration curve. Mitochondria remain

Table 5 | Antibody markers for western blot analysis (Step 32B(ii))

Antigen	Localization	Size (kDa)	Manufacturer, cat. no.	RRID	Dilution	Application
Actin	Cytosol	42	Sigma, cat. no. A2228	AB_476697	1: 4,000	Purity
Lamin B1	Nucleus	70	Abcam, cat. no. ab16048	AB_443298	1: 1,000	Purity
GFP	OMM	31	Santa Cruz, cat. no. sc-9996	AB_627695	1: 500	IP and purity
Tomm20	OMM	16	Abcam, cat. no. ab78547	AB_2043078	1: 1,000	IP and purity
VDAC1	OMM	39	Abcam, cat. no. ab14734	AB_443084	1: 1,000	IP and purity
ATP5a	IMM	55	Abcam, cat. no. ab14748	AB_301447	1: 10,000	IP and purity
CypD	Matrix	21	Abcam, cat. no. ab110324	AB_10864110	1: 5,000	IP and purity

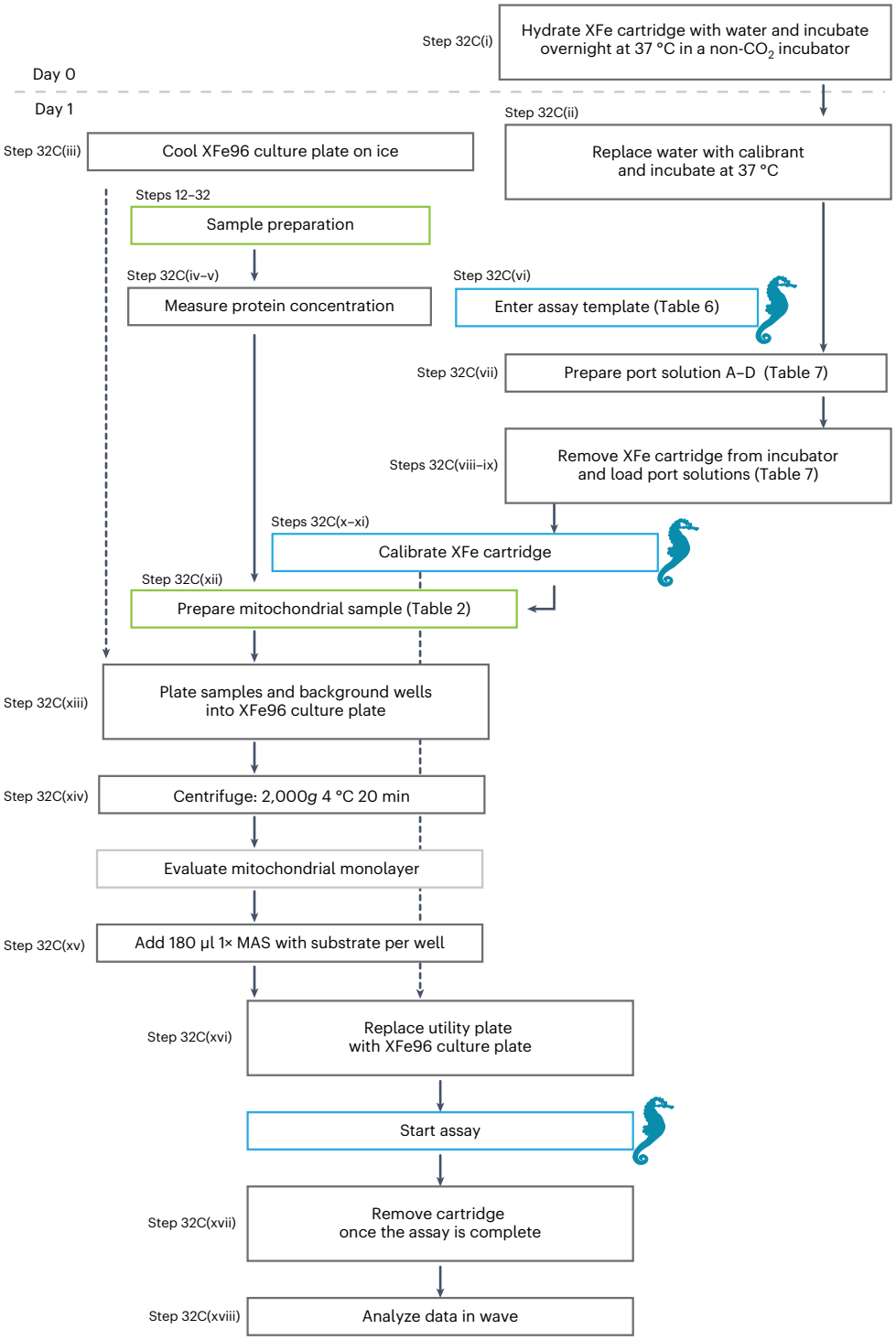

Fig. 6 | Outline of Step 32C to functionally probe mitochondrial bioenergetics via the Seahorse analyzer. Note that the XFe cartridge needs to be hydrated 1 day before the isolation in a non-CO_2 incubator. Steps performed with the Seahorse analyzer are indicated in blue (seahorse sign) and those involving mitochondria preparation are indicated in green. Reagent and sample amount information is given in Tables 2, 6 and 7.

viable at high concentrations (e.g., 10 mg/ml). The volume for resuspension depends on the pellet size and should be as small as possible (e.g., ~50 µl for CNS tissues and 100–200 µl for liver).

? TROUBLESHOOTING

Table 6 | Assay setting template (Step 32C(vi))

Step	Command	Time (min)	Repeat	Port
Initialization	Calibration	Auto	—	No injection
	Equilibration	Auto	—	
Basal	Mix	1:00	1×	No injection
	Wait	0:00		
	Measure	3:00		
Injection A	Mix	1:00	1×	A
	Wait	0:00		
	Measure	3:00		
Injection B	Mix	1:00	1×	B
	Wait	0:00		
	Measure	3:00		
Injection C	Mix	1:00	1×	C
	Wait	0:00		
	Measure	3:00		
Injection D	Mix	1:00	1×	D
	Wait	0:00		
	Measure	3:00		
Total time:		20:00		

Table 7 | Port solutions for mitochondrial stress test (Step 32C(vii))

Port	Volume	Compound	10× Port solution	Final concentration
A	20 µl	ADP	40 mM	4 mM
B	22 µl	Oligomycin A	15 µM	1.5 µM
C	25 µl	CCCP	(10×)[a]	[a]
D	27 µl	Antimycin A + Rotenone	40 µM	4 µM
			20µM	2 µM

[a]See Table 2 for tissue-dependent information.

(vi) Enter the template assay design with five to eight technical replicates per condition and define the instrument settings in the XFe96 Analyzer software as outlined in Table 6. To reduce the time, this step can be prepared the day before.

(vii) Prepare the port injection solutions in 1× MAS buffer as outlined in Table 7 using a 2× MAS stock. For a full XFe96 plate, prepare 3 ml injection solution for each compound. Calculate the corresponding volume from the compound stock solution to reach the final concentration of 10× compound in 1× MAS. For example, for ADP add 300 µl of 400 mM ADP to 2.7 ml of 1x MAS to reach a final concentration of 40 mM ADP/1× MAS.

▲ **CRITICAL STEP** Port solutions are prepared and loaded into the cartridge at 10× concentration and will reach the final concentration once injected during the assay. BSA should not be included in this solution since it facilitates bubble formation and increases the chance of port injection failure.

(viii) Remove the cartridge from the incubator and position it with the triangular notch at the bottom left-hand corner.

(ix) With a multichannel pipette, load each port of the cartridge with the respective 10× port solution A to D and the indicated volume in Table 7.

? TROUBLESHOOTING

(x) In the XFe96 Analyzer software, activate run and the instrument tray will be ejected.

(xi) Place the loaded cartridge and utility plate into the instrument tray and click 'I'm ready' to start calibration of sensors. This step takes ~15–30 min.

▲ **CRITICAL STEP** The triangular notch must be positioned at the bottom left-hand corner. Make sure the cartridge is seated properly in the tray.

(xii) During the calibration processes, prepare the mitochondrial sample from Step 32C(i) according to the amount and the specific substrate for the assay to be performed. For each measurement, mitochondrial sample in a volume of 10 µl is needed in five to eight technical replicates. Prepare a master mix based on the number of technical replicates per condition and the µg of protein suggested for individual ICs (Table 2) in 1× MAS buffer with substrate on ice. For example, for probing complex I in cortical mitochondria prepare eight replicates of 2 µg protein; 8 × 2 µg = 16 µg protein in 80 µl 1× MAS buffer with 10 mM pyruvate and 2 mM malate.

▲ **CRITICAL STEP** It is essential for mitochondria to be already diluted in buffer containing the substrates to prevent damage or loss of respiratory activity during the following centrifugation.

(xiii) Plate 10 µl of the master mix containing mitochondria into the wells of the cooled Agilent Seahorse XFe96 Cell Culture Microplate from Step 32C(v). Fill at least four wells with 10 µl 1× MAS buffer with substrate only (no mitochondria) for background correction.

▲ **CRITICAL STEP** The small volume per well is necessary to pellet mitochondria as a consistent monolayer onto the well bottom.

(xiv) Centrifuge the plate at 2,000*g* at 4 °C for 20 min to pellet mitochondria onto the well bottom. After the centrifugation, visualize mitochondria on the well bottom using a light microscope with a 20× or 40× air objective. Take a note of wells in which the mitochondrial monolayer is not formed or disrupted.

▲ **CRITICAL STEP** Use a fast acceleration and slow brake settings for centrifugation to avoid uneven mitochondrial distribution at the bottom of the plate due to sudden deceleration.

(xv) Once completed, dispense 180 µl 1× MAS with the respective substrate to each well, including background wells. Keep the plate on ice.

(xvi) After the sensor calibration is completed (Step 32C(xi)), replace the utility plate with the Agilent XFe96 Cell Culture Microplate containing the samples, and click 'I'm ready' to start the assay.

(xvii) Remove the sensor cartridge along with the Agilent XFe96 Cell Culture Microplate after the assay is completed.

(xviii) Perform data analysis on the Agilent Seahorse Wave desktop software or using the Seahorse Analytics website (https://seahorseanalytics.agilent.com/Account/Login). It is important to identify outliers due to injection failure or uneven distribution of mitochondria and exclude wells that did not respond accordingly to the injection. As outlined in Table 6, the assay starts with basal measurements. Next, the addition of ADP fuels ATP synthase (complex V) leading to an increase in oxygen consumption ratio (OCR). The second injection with oligomycin A inhibits complex V and impacts the electron flow-through the electron transport chain, resulting in less ATP production, lower mitochondrial respiration and a decrease in OCR. Third, addition of the mitochondrial uncoupler CCCP leads to maximal mitochondrial respiration caused by mitochondrial membrane depolarization. Finally, the combination of antimycin A (complex III inhibitor) and rotenone (complex I inhibitor) leads to the shut down of mitochondrial respiration. Mitochondrial respiration should respond as described above for the individual compounds and indicates the isolation of functional and well respiring mitochondria. With this injection strategy, the following parameters can be calculated: (1) basal respiration (State II), which is used to drive ATP synthesis, and represents the mitochondrial respiration in the presence of substrates but without ADP; (2) the ADP-stimulated respiration (State III), which corresponds to the formation of ATP from ADP and inorganic phosphate; (3) the non-ADP-stimulated respiration (State IV_o), representing the proton leak observed from the inhibition of the ATP synthase by oligomycin A; and (4) the maximal respiration (State IIIu) after CCCP addition. All parameters are calculated after subtracting the OCR values obtained after the injection of rotenone and antimycin A (non-mitochondrial O_2 consumption). Besides that, the respiratory control ratio, defined as the ratio of state III: state IV_o, is commonly used as an index of the integrity and coupling state of the mitochondria[34,61].

? TROUBLESHOOTING

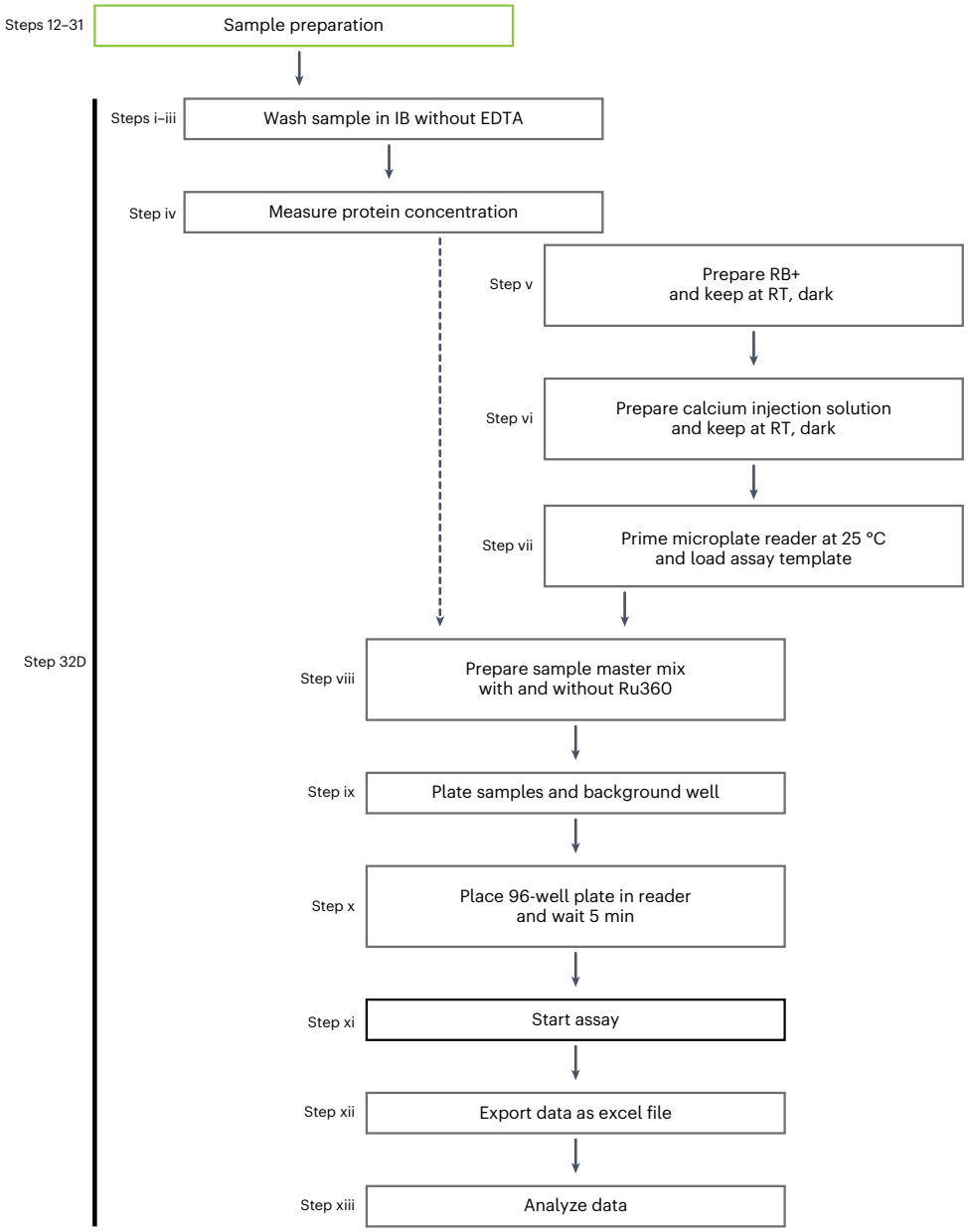

Fig. 7 | Outline of Step 32D to functionally probe for mitochondrial Ca^{2+} uptake ex vivo. Mitochondrial Ca^{2+} is measured via a fluorescence microplate reader assay using CalciumGreen-5N. This cell-impermeable dye informs about the extramitochondrial calcium concentration during the assay. Note that CalciumGreen-5N containing buffers should be kept in the dark and that the assay requires a constant temperature ≥25 °C. Steps involving mitochondria preparation are indicated in green.

(D) **Assays probing for mitochondrial functions: mitochondrial Ca^{2+} uptake assay**

● **Timing 60 min**

▲ **CRITICAL** For protocol outline, see Fig. 7.

(i) Resuspend the pellet from Step 31 in 1 ml IB without EDTA

▲ **CRITICAL STEP** EDTA will interfere with the Ca^{2+} update assay.

(ii) Centrifuge at 8,000*g* at 4 °C for 3 min and discard the supernatant.

(iii) Resuspend the pellet gently in a small amount of IB with 0.2% BSA but without EDTA.

▲ **CRITICAL STEP** Immunocaptured mitochondria should be used for functional assays within 1–2 h for best performance.

(iv) Quantify the protein concentration of samples by BCA protein assay or other protein quantification methods (e.g., 660 nm Protein Assay). Test several dilution factors of the

sample (25×, 50× and 100×) in triplicates to obtain an accurate sample concentration.
▲ **CRITICAL STEP** For reproducible results, be sure to use the same quantification method for all samples and the same standard for the calibration curve. Mitochondria remain viable at high concentrations (e.g., 10 mg/ml). The volume for resuspension depends on the pellet size and should be as small as possible (e.g., ~50 µl for CNS tissues and 100–200 µl for liver).
? TROUBLESHOOTING

(v) Prepare the supplemented respiration buffer (RB+) and protect the solution from light. CalciumGreen-5N is a non-membrane permeable Ca^{2+} indicator, which cannot enter intact mitochondria and has a K_d of 14 µM.

(vi) Prepare the calcium injection solution.
▲ **CRITICAL STEP** Protect the solution from light and keep at RT.

(vii) In a microplate reader with injector (for example, BMG Labtech, Clario star), set the temperature control to 25 °C and prime the syringe with calcium injection solution.

(viii) For each measurement, use at least 50 µg of mitochondrial sample in a volume of 90 µl RB+. Prepare a master mix for three to five technical replicates with either 10 µM Ru360 or ultrapure water, and gently mix. Ru360 is a known inhibitor of the Mcu and blocks mitochondrial Ca^{2+} uptake.

(ix) Disperse 90 µl of each master mix containing 50 µg mitochondrial ± Ru360 into the wells of a black, optical bottom 96-well plate. Fill three wells with 90 µl RB+ without mitochondria for background correction.

(x) Place the loaded 96-well plate into the microplate reader, close and wait for 5 min.

(xi) Start the assay and measure fluorescence with excitation at 485 nm and emission at 530 nm, every 2 s for a total of 24 min. Injections of 20 µM $CaCl_2$ in RB+ are performed every 3 min to a total of eight injections.

(xii) Export the measurements to an Excel file.

(xiii) Calculate the calcium uptake capacity as the differential area under the curve (ΔAUC) between the presence and absence of Ru360 (Fig. 5e). Ignore the first $CaCl_2$ injection because of residual EDTA present in the isolation. Background correct and normalize traces to the injection timepoint, and calculate the AUC. Display the difference between AUC_{-Ru360} and AUC_{+Ru360} per sample (ΔAUC) as percentage of AUC_{+Ru360}.

Troubleshooting

Troubleshooting advice can be found in Table 8.

Table 8 | Troubleshooting table

Step	Problem	Possible reason	Solution
3A(iv)	No PCR-positive mice in multiple litters	False-negative PCR result	Test tissue for expression by microscopy and optimize PCR protocol
		Genetics of parents	If multiple negative litters are observed, change breeding pair
3A(xiv), 3B(vi), 11	MitoTag expression in off-target cells	Germline recombination	Change Cre-driver mouse line; keep line as recommended in the literature; avoid using recombined animals as breeders
			Whole-animal recombination can be excluded with PCR strategies probing the CMV promoter and GFP-OMM sequence
		Genetic drift of the Cre-driver line	Obtain new founder for Cre-driver line from repository
	Low MitoTag expression	Inefficient recombination, for example in tamoxifen-inducible Cre-driver lines	Optimize induction protocol or change Cre-driver line
		Inefficient delivery of AAV virus	Optimize neonatal injection protocol. Obtain new viral batch and store viral vectors according to recommendations

Table continued

Table 8 (continued)

Step	Problem	Possible reason	Solution
	No GFP signal	Antigen masked by fixation method	Use heat-mediated antigen retrieval as outlined in ref. [6]
	Inconsistent GFP signal in cell processes	Antigen masked by tissue architecture, for example, mitochondria in myelinated axons	Use heat-mediated antigen retrieval as outlined in ref. [6] or consider alternative permeabilization approaches
12	Perfusion cannot be performed for tissue of interest	Tissue cannot be well perfused with standard protocol or perfusion time is too long. As a result, blood contamination in mitochondrial isolations can impair organelle function and proteomics analysis	Replace perfusion by extensive mincing and washing steps to remove blood contamination in tissues
16	Incomplete homogenization	Nonoptimal tissue grinder size and cycle number	Adjust the pestle size and optimize the number of up-and-down cycles (Table 4 and Extended Data Fig. 3)
	Broken mitochondria	Pestle too big, too many up-and-down cycles and/or incorrect speed	Adjust pestle size, use 300 rpm and five cycles for soft tissues. This step homogenizes the tissue to a single-cell suspension and should not break/lyse cells
19	Cell disruption vessel not available	—	Alternatively, cells can be ruptured by a Dounce homogenizer at higher rpm and longer time. Perform this step in a cold room to reduce heat production
	Incomplete homogenization	Incubation in cell disruption vessel too short	Adjust the time depending on sample volume
	Broken mitochondria	Pressure during incubation too high	Use 800 psi and regulate pressure through valve A (Fig. 3b, right, green), if accidently a higher pressure was applied
	Incomplete cell lysis	Pressure during incubation too low	Adjust the pressure to 800 psi after ~30 s. Gas can be absorbed by the solution
26	Buffer does not exit the column by gravity	Defective LS column	Replace column. Do not try to force buffer through column
	Slow column flow	Cell debris blocking the column	Perform again the first part of Step 22: pass tissue lysate through a 30 µm cell strainer to remove remaining cell debris
		Air bubble formation within the column	Degas ICB+ using vacuum and a sonication water bath, or prepare buffer the day before the experiment to allow degassing
30	Low yield of immunocaptured mitochondria	Nonoptimal IC incubation time	Optimize the incubation time dependent on GFP-OMM abundance in sample
		Nonoptimal input for IC	Optimize the amount of tissue lysate used per IC dependent on GFP-OMM abundance in sample
		Nonoptimal amount of microbeads used for IC	Optimize the amount of microbeads used per IC dependent on GFP-OMM abundance in sample
	Low respiratory competence of immunocaptured mitochondria	Incubation time for IC too long	Reduce the incubation time and modify the IC parameters: input amount and microbead volume
32A(v)	Low signal in LC–MS runs	Low abundance sample	Use sample preparation methods that are optimized for small samples, such as single-pot, solid-phase-enhanced sample preparation, SP3 (ref. [60])
	High contamination with non-mitochondrial proteins	Insufficient sample washes	Increase washes with IB+. Gently resuspend mitochondria before the centrifugation steps (Steps 29–31)
			Consider control isolation from wild-type tissue to test nonspecific binding to microbeads or control IC with mouse-IgG_1 antibodies
			Optimize IC conditions (input concentration and amount, microbead volume and incubation time) and test mitochondrial purity via western blot analysis
	Signal interference	DNA contamination in sample	Degrade DNA during the sample preparation using sonication and/or benzonase treatment

Table continued

Table 8 (continued)

Step	Problem	Possible reason	Solution
32C(ii)	High contamination with nontagged mitochondria	Tissue lysate is too concentrated	Generate a lysate of 20 mg tissue/ml and use a concentration of 2 mg/ml during the IC
	Low yield of immunocaptured mitochondria	MitoTag crossing has changed expression	Check expression via microscopy and alter breeding if needed
		Low abundant cell type within tissue	Increase IC material applied per LC column (e.g., 5× ICs on one column) and pool multiple animal per experiment to achieve the necessary material for downstream assay
		Damaged mitochondria	Prepare the tissue homogenate with care to avoiding damage to the mitochondria (Step 16). Perform all steps on ice or in cold room and pre-chill buffers before use
		Incubation time too short	Increase time depending on the abundance of tagged mitochondria present in the tissue lysate
	Poor mitochondria viability	Mitochondria too diluted	Keep the dilution ratios at 2mg/ml. If working with limiting tissue, it may be necessary to pool mice or reduce the IB+ volume used (Step 15)
		Too many beads are used for too few mitochondria	Adjust microbeads volume to the abundance of tagged mitochondria present in the tissue lysate
		Incubation time was too long	Adjust incubation time at 4 °C to the necessary amount depending on the abundance of tagged mitochondria present in the tissue lysate. If too few tagged mitochondria are present, increase the lysate amount used per IC column
32C(ix)	Port injection failure	Improper loading of port solution or bubble formation	Carefully follow the port loading guide provided with the Sensor Cartridge
32C(xviii)	Noise background	Bubble formation during hydration	Tap the plate a few times to break down possible bubbles that have formed
32C(xviii)	High variability among technical replicates	Improper loading of port solution	Carefully follow the port loading guide provided with the Sensor Cartridge
32C(xviii)	Low OCR respiration	Poor mitochondria viability during IC	Adjust the initial tissue lysate concentration (Step 15) and the lysate dilution during IC incubation (Steps 23–24)
		Too little or too much mitochondria per well	For each tissue source, perform pilot experiments to titrate the mitochondrial amount needed
	Low response to CCCP	CCCP concentration too low or too high	For each tissue source, perform pilot experiments to titrate the CCCP amount needed
		CCCP stock impaired	When preparing a new CCCP stock, test its efficiency compared with the previous stock. Aliquot in appropriate amounts and do not freeze again after use

Timing

Steps 1–3, cell-type-specific expression of GFP-OMM using MitoTag reporter mice: 6–8 weeks (excluding mouse line import)
Steps 4–11, validation of cell-type-specific GFP-OMM expression: 3–4 days
Steps 12–22, mouse killing, tissue homogenization and plasma membrane permeabilization: 30 min per animal
Steps 23–31, IC of cell-type-specific mitochondria: 90 min
Step 32C, measurements of mitochondrial bioenergetics with Seahorse analyzer: 90–120 min
Step 32D, mitochondrial Ca^{2+} uptake assay: 60 min

Anticipated results

If MitoTag expression is confirmed, the described protocol results in the isolation of sufficient amounts of functional mitochondria from a specific cell type in vivo that was defined by Cre-recombinase expression.

As one might expect, the mitochondria yield is directly proportional to the abundance of the respective cell type and their mitochondria in a given tissue; still, from our experience, a sufficient amount of mitochondria can be isolated even from relatively low abundance cell types (cholinergic neurons from cortex and spinal cord; Fig. 5a). On the basis of our work in cerebellum[6], we have obtained per mg initial tissue ~2.5 µg mitochondria from Purkinje cells, the major cerebellar inhibitory neuron; ~1.3 µg mitochondria from astrocytes, and ~4.3 µg mitochondria from granule cells, the most abundant cerebellar excitatory neuron. Thus, depending on the cell type, between ~100 and 350 µg of mitochondria can be isolated from one mouse cerebellum (~90 mg). Overall, for a tissue of this size and its medium-to-high abundance cell types, this amount is sufficient to perform a number of downstream analyses from a single mouse, allowing individual animals as biological replicates. Most importantly, this amount allows in-depth proteomic analysis with routine label-free quantification yielding quantifications for up to 3,718 proteins[6] and a 68% coverage of MitoCarta 2.0 proteins[62]. Intensity-based absolute quantification revealed a strong enrichment for mitochondrial proteins over non-mitochondrial proteins in IC (see Fecher et al.[6], Supplementary Fig. 3c,d). Among non-mitochondrial proteins, proteins with localization in cytosol and nucleus were most abundant[6].

Beyond yield, other key parameters are purity and specificity of the IC, which are not easy to assess, as both enrichment of mitochondria in general and of the respective cell-type-specific subpopulation have to be determined. For analyzing mitochondrial purity, routine western blot techniques can be used, where it is expected to see a reduction in cytosolic markers (e.g., Actb) in the mitochondrial fraction and an enrichment of mitochondrial markers. To ensure that intact mitochondria and not mitoplasts are enriched, these markers cover ideally all compartments of a mitochondrion: OMM, inner mitochondrial membrane (IMM) and mitochondrial matrix (e.g., for OMM: VDAC, Tom20; for IMM: ATP5A; for matrix: CypD; Table 5). In principle, also quantification of mitochondrial DNA could provide a further measurement of enrichment, especially if subsequent sequencing is the aim. Typically, an enrichment of mitochondrial markers in the IC over the input (PNL after homogenization, nitrogen cavitation and cell debris removal; Step 22) of several fold can be expected. This enrichment is higher for other purification methods, such as density gradient centrifugation[35]. Specificity, i.e., the selective enrichment of mitochondria from the target cell type during the IC, can be evaluated via the ratio of GFP-OMM (as marker for the tagged population of mitochondria) and endogenous mitochondrial markers. Note that in some purifications, also a fraction of free GFP without the OMM anchor (i.e., 27 kDa versus 31 kDa for GFP-OMM) can be detected, which is formed during the isolation due to enhanced pipetting and shear stress on the OMM. Western blot analysis can be used to compare the initial CMF with the IC against GFP (IC GFP) and the tissue background IC using anti-Tom22 microbeads (IC Tom). Further information about the efficacy of the IC can be gathered by analyzing the flow-through of IC GFP (FT mito). It is expected to see an enrichment of GFP-OMM in the IC GFP sample, while the GFP content should be unchanged in the IC Tom and depleted in FT mito when compared with the initial CMF. To make this comparison meaningful, all samples should be normalized to mitochondrial mass using a set of mitochondrial markers. It has to be kept in mind that enrichment factors have a ceiling dependent on the mitochondrial abundance of the target cell type. For example, if one-third of tissue mitochondria are labeled, a maximal enrichment factor of three can be achieved.

Notably, in our experience, even moderately enriched proteins in proteomic comparisons between cell types can prove to be highly specific mitochondrial cell type markers when visualized in situ using immunofluorescence (e.g., Mcu for granule cells and Rmdn3 for Purkinje cells in cerebellum[6]). Indeed, while in our experience, enrichment parameters measured on isolated mitochondria correlate between mass spectrometry and western blot analysis, it cannot be anticipated that there is a simply quantitative correspondence between these measures and in situ immunofluorescence quantifications that are also affected by organelle geometry, antibody access and non-linearity of fluorescence detection.

Finally, downstream assays of mitochondrial function inform about the viability of IC isolates (e.g., oxygen consumption via the Seahorse analyzer)[63]. Here, the respiratory control ratio is commonly used as an index of the integrity and coupling state of mitochondria[35]. In our hands, an acceptable value for this state III/IV_o ratio is >5, regardless of the cell-type-specific mitochondria probed and the substrates utilized (e.g., pyruvate/malate for complex I, succinate/rotenone for complex II or $_L$-palmitoyl/carnitine for beta-oxidation). Besides that, mitochondrial respiration should follow the general pattern of (1) an increase in OCR after ADP injection, (2) a decrease after oligomycin A injection, and (3) an increase after CCCP injection. Finally, (4) we expect to see a drop to almost 0 pmol/min with rotenone and antimycin A injection, as these reagents block all mitochondrial

respiration. Only traces that follow this general pattern (Fig. 5b) are indicative of viable mitochondria and should be considered. Obviously, in specific samples—e.g., mitochondria isolated from affected cell types in a disease model—deviations could indicate pathophysiology rather than a technical problems with the isolation process. Therefore, suitable control samples (e.g., IC Tom) need to be included in every experiment. Similar rules apply to Ca^{2+} uptake measurements (Fig. 5c,d), where physiologically intact and coupled mitochondria should uptake multiple calcium pulses before mitochondrial permeability transition pore opening[64].

In general, the user can anticipate from this protocol a robust and reproducible IC of viable mitochondria with consistent yield among experiments. Depending on the intended downstream assays, increasing the amount of tissue per column and/or the amount of microbeads used can increase mitochondrial yield. Alternatively, more samples might be processed or tissue from multiple mice might be pooled, before downstream analyses are performed. With such modifications, a wide range of multiparametric analyses, even beyond those detailed here, should be possible that allow interested researchers to characterize in-depth how mitochondria differ between cell types in a given tissue, developmental stage or disease process.

Reporting summary

Further information on research design is available in the Nature Portfolio Reporting Summary linked to this article.

Data availability

Data presented in this article have been previously published and associated raw data are provided in the related article[6].

References

1. Pagliarini, D. J. & Rutter, J. Hallmarks of a new era in mitochondrial biochemistry. *Genes Dev.* **27**, 2615–2627 (2013).
2. Pagliarini, D. J. et al. A mitochondrial protein compendium elucidates complex I disease biology. *Cell* **134**, 112–123 (2008).
3. Nunnari, J. & Suomalainen, A. Mitochondria: in sickness and in health. *Cell* **148**, 1145–1159 (2012).
4. Weinberg, S. E., Sena, L. A. & Chandel, N. S. Mitochondria in the regulation of innate and adaptive immunity. *Immunity* **42**, 406–417 (2015).
5. Motori, E. et al. Neuronal metabolic rewiring promotes resilience to neurodegeneration caused by mitochondrial dysfunction. *Sci. Adv.* **6**, eaba8271 (2020).
6. Fecher, C. et al. Cell-type-specific profiling of brain mitochondria reveals functional and molecular diversity. *Nat. Neurosci.* **22**, 1731–1742 (2019).
7. Bayraktar, E. C. et al. MITO-tag mice enable rapid isolation and multimodal profiling of mitochondria from specific cell types in vivo. *Proc. Natl Acad. Sci. USA* **116**, 303–312 (2019).
8. Barros, L. F. et al. Current technical approaches to brain energy metabolism. *Glia* **66**, 1138–1159 (2018).
9. Misgeld, T. & Schwarz, T. L. Mitostasis in neurons: maintaining mitochondria in an extended cellular architecture. *Neuron* **96**, 651–666 (2017).
10. Plucinska, G. & Misgeld, T. Imaging of neuronal mitochondria in situ. *Curr. Opin. Neurobiol.* **39**, 152–163 (2016).
11. Pekkurnaz, G. & Wang, X. Mitochondrial heterogeneity and homeostasis through the lens of a neuron. *Nat. Metab.* **4**, 802–812 (2022).
12. Bomba-Warczak, E., Edassery, S. L., Hark, T. J. & Savas, J. N. Long-lived mitochondrial cristae proteins in mouse heart and brain. *J. Cell Biol.* **220**, e202005193 (2021).
13. Sanz, E. et al. Cell-type-specific isolation of ribosome-associated mRNA from complex tissues. *Proc. Natl Acad. Sci. USA* **106**, 13939–13944 (2009).
14. Franko, A. et al. Efficient isolation of pure and functional mitochondria from mouse tissues using automated tissue disruption and enrichment with anti-TOM22 magnetic beads. *PLoS One.* **8**, e82392 (2013).
15. Horie, C., Suzuki, H., Sakaguchi, M. & Mihara, K. Characterization of signal that directs C-tail-anchored proteins to mammalian mitochondrial outer membrane. *Mol. Biol. Cell* **13**, 1615–1625 (2002).
16. Chen, W. W., Freinkman, E., Wang, T., Birsoy, K. & Sabatini, D. M. Absolute quantification of matrix metabolites reveals the dynamics of mitochondrial metabolism. *Cell* **166**, 1324–1337.e1311 (2016).
17. Zambrowicz, B. P. et al. Disruption of overlapping transcripts in the ROSA beta geo 26 gene trap strain leads to widespread expression of beta-galactosidase in mouse embryos and hematopoietic cells. *Proc. Natl Acad. Sci. USA* **94**, 3789–3794 (1997).
18. Meeusen, S., McCaffery, J. M. & Nunnari, J. Mitochondrial fusion intermediates revealed in vitro. *Science* **305**, 1747–1752 (2004).
19. Breckwoldt, M. O. et al. Multiparametric optical analysis of mitochondrial redox signals during neuronal physiology and pathology in vivo. *Nat. Med.* **20**, 555–560 (2014).

20. Fecher, C. *Mitochondrial Diversity Probed in Mouse Cerebellum Elucidates Cell Type-Specific Fine-Tuning of Mitochondrial Biology*. PhD thesis, LMU München (2020).
21. Wynne, M. E. et al. Heterogeneous expression of nuclear encoded mitochondrial genes distinguishes inhibitory and excitatory neurons. *eNeuro*. https://doi.org/10.1523/eneuro.0232-21.2021 (2021).
22. das Neves, R. P. et al. Connecting variability in global transcription rate to mitochondrial variability. *PLoS Biol.* **8**, e1000560 (2010).
23. Medini, H., Cohen, T. & Mishmar, D. Mitochondrial gene expression in single cells shape pancreatic beta cells' sub-populations and explain variation in insulin pathway. *Sci. Rep.* **11**, 466 (2021).
24. Hubbard, W. B. et al. Fractionated mitochondrial magnetic separation for isolation of synaptic mitochondria from brain tissue. *Sci. Rep.* **9**, 9656 (2019).
25. Suomalainen, A. & Battersby, B. J. Mitochondrial diseases: the contribution of organelle stress responses to pathology. *Nat. Rev. Mol. Cell Biol.* **19**, 77–92 (2018).
26. De Stefani, D., Rizzuto, R. & Pozzan, T. Enjoy the trip: calcium in mitochondria back and forth. *Ann. Rev. Biochem.* **85**, 161–192 (2016).
27. Ahier, A., Onraet, T. & Zuryn, S. Cell-specific mitochondria affinity purification (CS-MAP) from *Caenorhabditis elegans*. *STAR Protoc.* **2**, 100952 (2021).
28. Harbauer, A. B. et al. Neuronal mitochondria transport Pink1 mRNA via synaptojanin 2 to support local mitophagy. *Neuron* **110**, 1516–1531.e1519 (2022).
29. Hansen, F. M. et al. Mitochondrial phosphoproteomes are functionally specialized across tissues. Preprint at *bioRxiv* https://doi.org/10.1101/2022.03.23.485457 (2022).
30. Cabrera-Orefice, A., Potter, A., Evers, F., Hevler, J. F. & Guerrero-Castillo, S. Complexome profiling-exploring mitochondrial protein complexes in health and disease. *Front. Cell Dev. Biol.* **9**, 796128 (2021).
31. Roh, H. C. et al. Simultaneous transcriptional and epigenomic profiling from specific cell types within heterogeneous tissues in vivo. *Cell Rep.* **18**, 1048–1061 (2017).
32. Bensley, R. R. & Hoerr, N. L. Studies on cell structure by the freezing-drying method V. The chemical basis of the organization of the cell. *Anat. Rec.* **60**, 251–266 (1934).
33. Hogeboom, G. H., Schneider, W. C. & Pallade, G. E. Cytochemical studies of mammalian tissues: I. Isolation of intact mitochondria from rat liver; some biochemical properties of mitochondria and submicroscopic particulate material. *J. Biol. Chem.* **172**, 619–635 (1948).
34. Frezza, C., Cipolat, S. & Scorrano, L. Organelle isolation: functional mitochondria from mouse liver, muscle and cultured filroblasts. *Nat. Protoc.* **2**, 287–295 (2007).
35. Sims, N. R. & Anderson, M. F. Isolation of mitochondria from rat brain using Percoll density gradient centrifugation. *Nat. Protoc.* **3**, 1228–1239 (2008).
36. Russo, G. L. et al. CRISPR-mediated induction of neuron-enriched mitochondrial proteins boosts direct glia-to-neuron conversion. *Cell. Stem Cell.* **28**, 524–534.e527 (2021).
37. Rath, S. et al. MitoCarta3.0: an updated mitochondrial proteome now with sub-organelle localization and pathway annotations. *Nucleic Acids Res.* **49**, D1541–D1547 (2021).
38. Alvarez-Castelao, B. et al. Cell-type-specific metabolic labeling of nascent proteomes in vivo. *Nat. Biotechnol.* **35**, 1196–1201 (2017).
39. Alvarez-Castelao, B., Schanzenbächer, C. T., Langer, J. D. & Schuman, E. M. Cell-type-specific metabolic labeling, detection and identification of nascent proteomes in vivo. *Nat. Protoc.* **14**, 556–575 (2019).
40. Smith, A. C. & Robinson, A. J. MitoMiner v4.0: an updated database of mitochondrial localization evidence, phenotypes and diseases. *Nucleic Acids Res.* **47**, D1225–D1228 (2019).
41. Benador, I. Y. et al. Mitochondria bound to lipid droplets have unique bioenergetics, composition, and dynamics that support lipid droplet expansion. *Cell Metab.* **27**, 869–885.e866 (2018).
42. Misgeld, T., Kerschensteiner, M., Bareyre, F. M., Burgess, R. W. & Lichtman, J. W. Imaging axonal transport of mitochondria in vivo. *Nat. Methods* **4**, 559–561 (2007).
43. Pham, A. H., McCaffery, J. M. & Chan, D. C. Mouse lines with photo-activatable mitochondria to study mitochondrial dynamics. *Genesis* **50**, 833–843 (2012).
44. Agarwal, A. et al. Transient opening of the mitochondrial permeability transition pore induces microdomain calcium transients in astrocyte processes. *Neuron* **93**, 587–605.e587 (2017).
45. MacDonald, J. A. et al. A nanoscale, multi-parametric flow cytometry-based platform to study mitochondrial heterogeneity and mitochondrial DNA dynamics. *Commun. Biol.* **2**, 258 (2019).
46. Cavelier, L., Johannisson, A. & Gyllensten, U. Analysis of mtDNA copy number and composition of single mitochondrial particles using flow cytometry and PCR. *Exp. Cell Res.* **259**, 79–85 (2000).
47. Fieni, F. et al. Voltage-dependent inwardly rectifying potassium conductance in the outer membrane of neuronal mitochondria. *J. Biol. Chem.* **285**, 27411–27417 (2010).
48. Zhang, S. et al. High-throughput multiparameter analysis of individual mitochondria. *Anal. Chem.* **84**, 6421–6428 (2012).
49. Luo, L. et al. Optimizing nervous system-specific gene targeting with Cre driver lines: prevalence of germline recombination and influencing factors. *Neuron* **106**, 37–65.e35 (2020).
50. Wanders, R. J. A., Waterham, H. R. & Ferdinandusse, S. Metabolic interplay between peroxisomes and other subcellular organelles including mitochondria and the endoplasmic reticulum. *Front. Cell Dev. Biol.* https://doi.org/10.3389/fcell.2015.00083 (2016).
51. Shai, N. et al. Systematic mapping of contact sites reveals tethers and a function for the peroxisome-mitochondria contact. *Nat. Commun.* **9**, 1761 (2018).

52. Herculano-Houzel, S. The glia/neuron ratio: how it varies uniformly across brain structures and species and what that means for brain physiology and evolution. *Glia* **62**, 1377–1391 (2014).
53. Sharma, K. et al. Cell type- and brain region-resolved mouse brain proteome. *Nat. Neurosci.* **18**, 1819–1831 (2015).
54. Murgia, M. et al. Proteomics of cytochrome c oxidase-negative versus positive muscle fiber sections in mitochondrial myopathy. *Cell Rep.* **29**, 3825–3834.e3824 (2019).
55. Schiaffino, S., Reggiani, C., Kostrominova, T. Y., Mann, M. & Murgia, M. Mitochondrial specialization revealed by single muscle fiber proteomics: focus on the Krebs cycle. *Scand. J. Med. Sci. Sports* **25**, 41–48 (2015).
56. Gella, A. et al. Mitochondrial proteome of affected glutamatergic neurons in a mouse model of leigh syndrome. *Front. Cell Dev. Biol.* **8**, 660 (2020).
57. Fünfschilling, U. & Reichardt, L. F. Cre-mediated recombination in rhombic lip derivatives. *Genesis* **33**, 160–169 (2002).
58. Davidson, B. L. & Breakefield, X. O. Viral vectors for gene delivery to the nervous system. *Nat. Rev. Neurosci.* **4**, 353–364 (2003).
59. Wang, M., Misgeld, T. & Brill, M. S. Neural labeling and manipulation by neonatal intraventricular viral injection in mice. *STAR Protoc.* **3**, 101081 (2022).
60. Hughes, C. S. et al. Single-pot, solid-phase-enhanced sample preparation for proteomics experiments. *Nat. Protoc.* **14**, 68–85 (2019).
61. Iuso, A., Repp, B., Biagosch, C., Terrile, C. & Prokisch, H. Assessing mitochondrial bioenergetics in isolated mitochondria from various mouse tissues using Seahorse XF96 analyzer. *Methods Mol. Biol.* **1567**, 217–230 (2017).
62. Calvo, S. E., Clauser, K. R. & Mootha, V. K. MitoCarta2.0: an updated inventory of mammalian mitochondrial proteins. *Nucleic Acids Res.* **44**, D1251–D1257 (2016).
63. Wettmarshausen, J. & Perocchi, F. Assessing calcium-stimulated mitochondrial bioenergetics using the Seahorse XF96 analyzer. *Methods Mol. Biol.* **1925**, 197–222 (2019).
64. Wettmarshausen, J. & Perocchi, F. Isolation of functional mitochondria from cultured cells and mouse tissues. *Methods Mol. Biol.* **1567**, 15–32 (2017).
65. Zambrowicz, B. P. et al. Disruption of overlapping transcripts in the ROSA βgeo 26 gene trap strain leads to widespread expression of β-galactosidase in mouse embryos and hematopoietic cells. *Proc. Natl Acad. Sci. USA* **94**, 3789–3794 (1997).
66. Daigle, T. L. et al. A suite of transgenic driver and reporter mouse lines with enhanced brain-cell-type targeting and functionality. *Cell* **174**, 465–480.e422 (2018).
67. Komatsu, M. et al. Loss of autophagy in the central nervous system causes neurodegeneration in mice. *Nature* **441**, 880–884 (2006).
68. Nectow, A. R. et al. Rapid molecular profiling of defined cell types using Viral TRAP. *Cell Rep.* **19**, 655–667 (2017).

Acknowledgements

We thank all authors of the related article[6] for their contribution to the establishment and validation of the MitoTag mouse model. Work in T.M.'s laboratory is supported by the DFG: CRC870 A11-ID 118803580, TRR 274/1 B03/ C02-ID 408885537, Mi 694/7-1, Mi 694/8-1, Mi 694/9-1 A03-ID 428663564, FOR ImmunoStroke and the ERC under the European Union's Seventh Framework Program (FP/2007-2013; ERC grant agreement no. 616791). T.M. is a member of and supported by the German Center for Neurodegenerative Diseases (DZNE) and by the Munich Center for Systems Neurology (SyNergy EXC 2145; Project ID 390857198). N.P.d.M. and C.F. were enrolled in the Munich Graduate School of Systemic Neurosciences (GSC 82–ID 24184143). Work in F.P.'s laboratory is supported by the Munich Center for Systems Neurology (SyNergy EXC 2145; Project ID 390857198) and the ExNet-0041-Phase2-3 ('SyNergy-HMGU') through the Initiative and Network Fund of the Helmholtz Association. The authors thank H.C. Delgado de la Herran, Y. Hufnagel and M. Feng for help with material and data collection.

Author contributions

N.P.d.M. and C.F. collected and analyzed the data. C.F. and N.P.d.M designed the figures with help from F.P. and T.M. A.M.P generated the video. All authors contributed to writing, editing and revision of the manuscript.

Competing interests

The authors declare no competing interests.

Additional information

Extended data is available for this paper at https://doi.org/10.1038/s41596-023-00831-w.

Supplementary information The online version contains supplementary material available at https://doi.org/10.1038/s41596-023-00831-w.

Correspondence and requests for materials should be addressed to Fabiana Perocchi or Thomas Misgeld.

Peer review information *Nature Protocols* thanks Elisenda Sanz and the other, anonymous, reviewer(s) for their contribution to the peer review of this work.

Reprints and permissions information is available at www.nature.com/reprints.

Publisher's note Springer Nature remains neutral with regard to jurisdictional claims in published maps and institutional affiliations.

Received: 12 August 2022; Accepted: 9 March 2023;
Published online: 16 June 2023

Related links
Key reference using this protocol
Fecher, C. et al. *Nat. Neurosci.* **22**, 1731–1742 (2019): https://doi.org/10.1038/s41593-019-0479-z

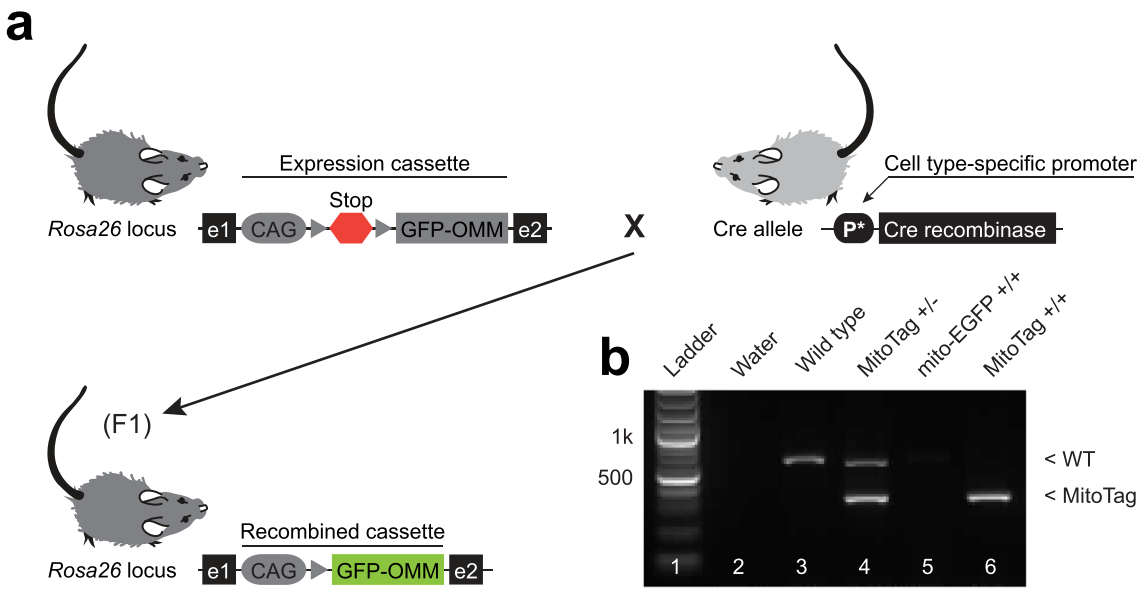

Extended Data Fig. 1 | MitoTag genetic strategy. a, MitoTag locus recombination within the endogenous Rosa26 locus occurs during the crossing of MitoTag mice with Cre-driver lines generating recombined animals (F1) that express GFP-OMM in Cre+ cells (green element). e1/2, exon 1/2; P*, cell-type-specific promoter. **b**, MitoTag PCR result demonstrating PCR primer specificity for the MitoTag allele. PCR products: wild-type Rosa26 locus (WT), ~600 bp (see lane 3); MitoTag transgene, 324 bp (see lane 6). Consult Step 3A(iv–xiii) for genotyping protocol. The Rosa26-tm4(CAG-EGFP*) reporter mouse is another Rosa26 knock-in model that Cre-conditionally expresses GFP localized to the mitochondrial matrix (mito-EGFP). Note the absence of PCR product in this homozygous sample in lane 5. Primers are specific for both alleles, GFP-OMM and the endogenous Rosa26 locus. The sample in lane 5 is from a homozygous Rosa26-tm4(CAG-EGFP*) mouse. A PCR against GFP would not discriminate between the two Rosa26 reporter mouse models. All animal experiments were approved by the responsible regulatory agencies (Regierung von Oberbayern). **a**, adapted from ref. [6], Springer Nature Ltd.

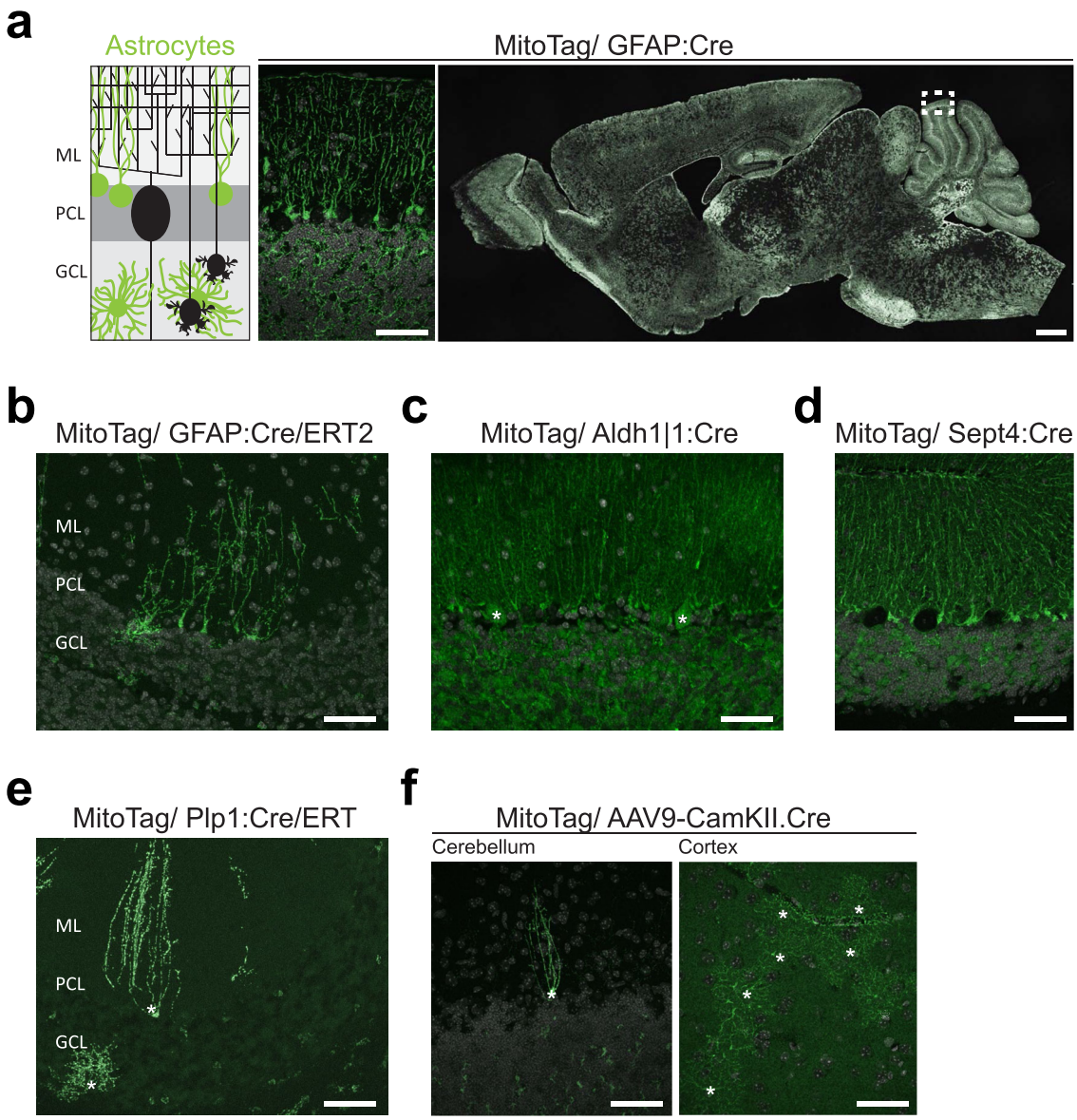

Extended Data Fig. 2 | MitoTag recombination in astrocytes through a number of Cre-driver lines and adeno-associated viral vector. a-f, MitoTag mice were recombined with different Cre-driver lines for the expression in astrocytes: **a**, mGFAP:Cre (77.6); **b**, hGFAP:CreERT2; **c**, Aldh1l1:Cre; **d**, Sept4:Cre; and **e**, Plp1:Cre/ERT; or neonatally injected with AAV9-CamkII.Cre virus (**f**, cerebellum and cortex). In cerebellum, two populations of astrocytes are present, namely Bergmann glia in the molecular layer (ML) with their cell body localized in the Purkinje cell layer (PCL) and protoplasmic astrocytes in the granule cell layer (GCL). Asterisks indicate leaky expression and off-target recombination. Scale bar, 1 mm for sagittal brain, 50 µm for detailed images. Further information on the Cre-driver lines is given in Table 1. All animal experiments were approved by the responsible regulatory agencies (Regierung von Oberbayern). **a**, adapted from ref. [6], Springer Nature Ltd.

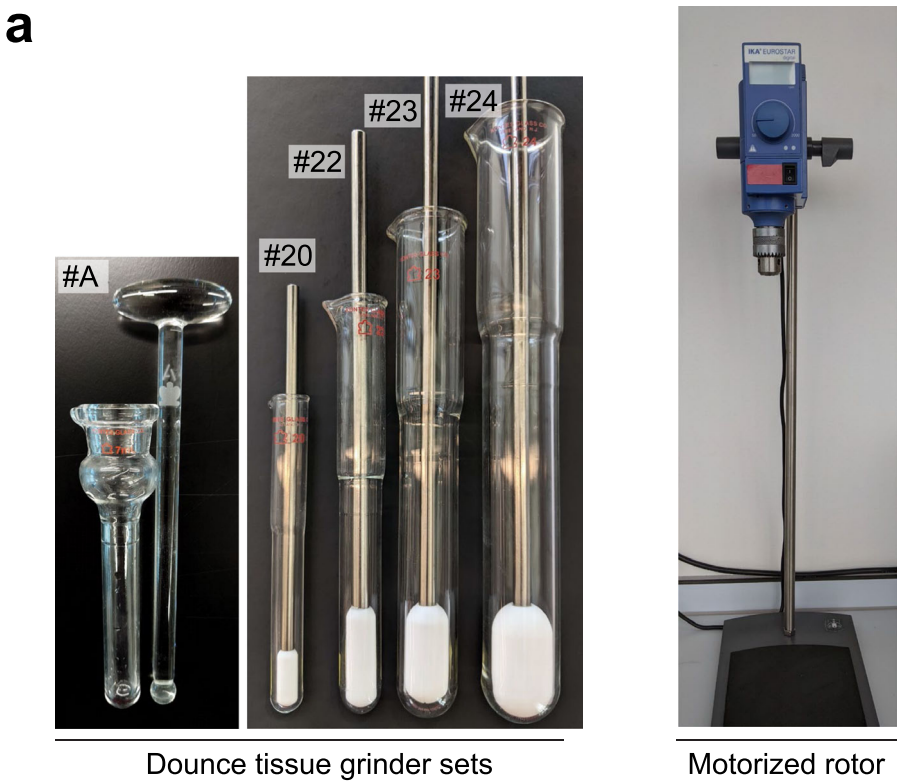

Extended Data Fig. 3 | Essential equipment for the tissue homogenization Step 16. a, Dounce glass tissue homogenizers of different sizes (volume and clearance, see Table 4). #A can be used for soft tissue and homogenization by hand, while #20, 22-24 are used in combination with a motorized rotor (300 rpm for the present protocol) and for different tissue sources (brain, liver, muscle tissue). **b**, Sample pictures illustrating the final immunocapture in Step 29 and 31. Note, final samples can vary in size and color between IC Tom and IC GFP dependent on the abundance of GFP-OMM tagged mitochondria in tissue lysate and the amount of microbeads used. Microbeads are present as dark central spot within the sample pellet and we have not observed adverse effects due to their presence in functional downstream assays. All animal experiments were approved by the responsible regulatory agencies (Regierung von Oberbayern).

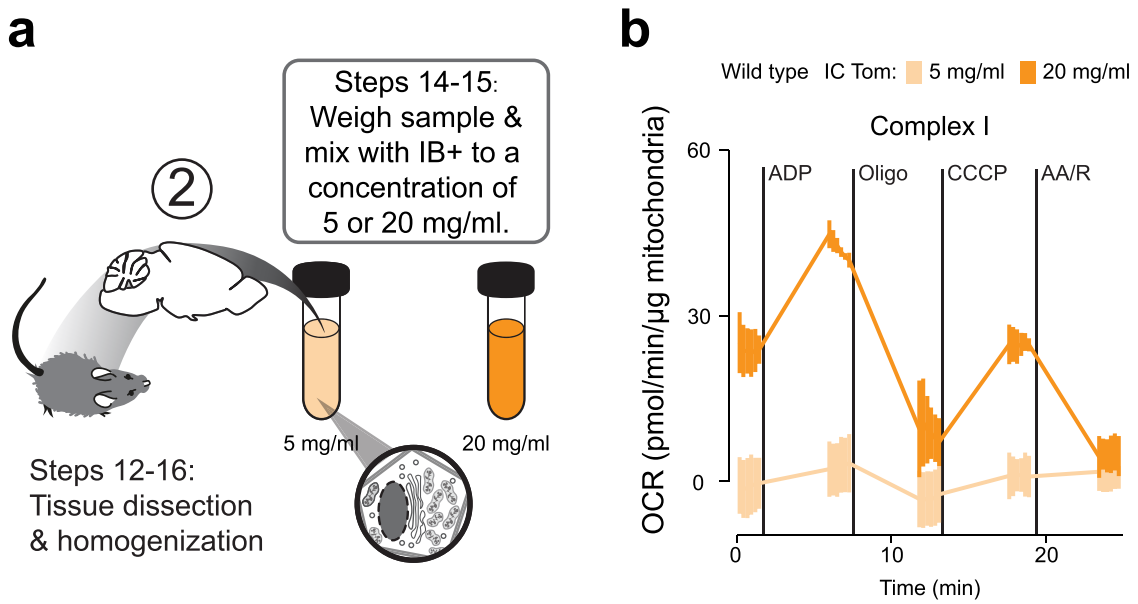

Extended Data Fig. 4 | Troubleshooting of mitochondrial viability via oxygen consumption rate (OCR) measurement. a, Protocol stage 2 illustrating the generation of a single-cell tissue homogenate in Step 16. For mitochondrial bioenergetics, two tissue lysate concentrations were generated in IB+: 5 mg/ml and 20 mg/ml, as recommended in our protocol. Immunocapture with IC Tom was performed from both samples as outlined in the PROCEDURE. **b**, Oxygen consumption ratio (OCR) via complex I (pyruvate/malate) from samples outlined in **a** (5 mg/ml, light orange; 20 mg/ml, orange) using 2 ug mitochondria/well supplemented with 10 mM pyruvate and 2 mM malate. The following compounds and concentrations were injected in the assay: ADP (4 mM), oligomycin A (Oligo, 1.5 µM), CCCP (10 µM), and rotenone (2 µM) together with antimycin A (4 µM; AA). The graph shows that mitochondrial functionality can be affected by the initial dilution during homogenisation, which is observed by the low OCR levels and unresponsiveness to the compounds of the 5 mg/ml sample (light orange) compared with the expected mitochondrial modulator responses of the standard sample (orange). Line graph: mean ± s.e.m. from ≥8 technical replicates. All animal experiments were approved by the responsible regulatory agencies (Regierung von Oberbayern).

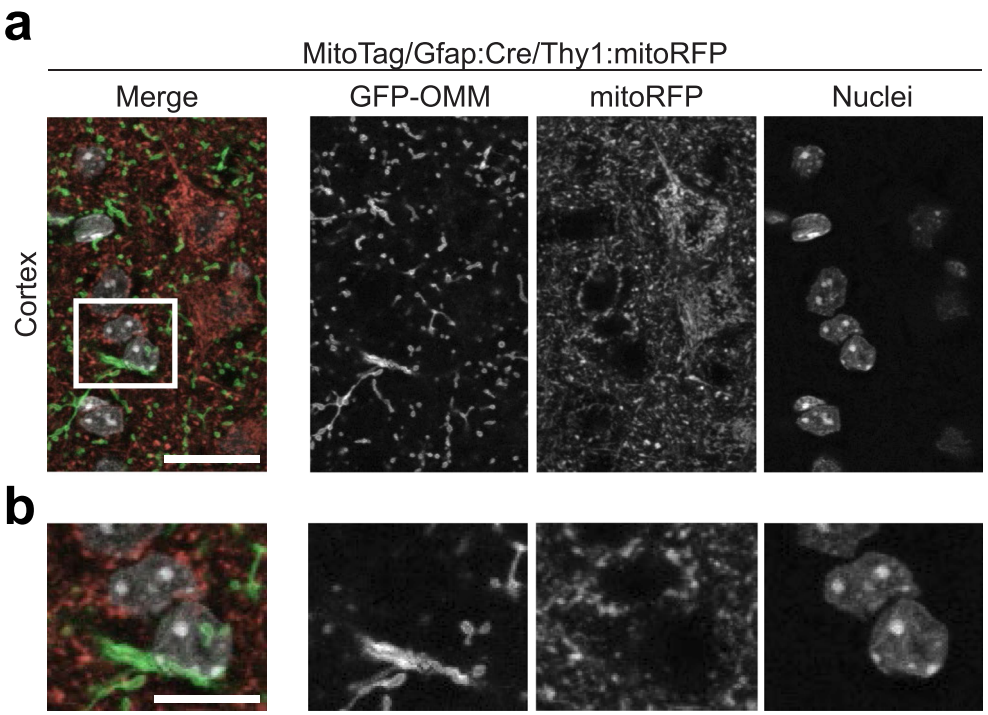

Extended Data Fig. 5 | Single-channel information from MitoTag/Gfap:Cre/Thy1:mitoRFP image represented in Fig. 4d. Cortex from MitoTag/Gfap:Cre/Thy1:mitoRFP animals used as tissue source in the 'spike-in' experiment. **a**, Merged image shown in Fig. 4d and corresponding single channels. **b**, Detail from **a**. Scale bar, 20 µm for **a**, 10 µm for **b**.

nature portfolio

Corresponding author(s): Fabiana Perocchi, Thomas Misgeld

Last updated by author(s): 2022-12-13

Reporting Summary

Nature Portfolio wishes to improve the reproducibility of the work that we publish. This form provides structure for consistency and transparency in reporting. For further information on Nature Portfolio policies, see our Editorial Policies and the Editorial Policy Checklist.

Please do not complete any field with "not applicable" or n/a. Refer to the help text for what text to use if an item is not relevant to your study.
For final submission: please carefully check your responses for accuracy; you will not be able to make changes later.

Statistics

For all statistical analyses, confirm that the following items are present in the figure legend, table legend, main text, or Methods section.

n/a Confirmed

- The exact sample size (*n*) for each experimental group/condition, given as a discrete number and unit of measurement
- A statement on whether measurements were taken from distinct samples or whether the same sample was measured repeatedly
- The statistical test(s) used AND whether they are one- or two-sided
  Only common tests should be described solely by name; describe more complex techniques in the Methods section.
- A description of all covariates tested
- A description of any assumptions or corrections, such as tests of normality and adjustment for multiple comparisons
- A full description of the statistical parameters including central tendency (e.g. means) or other basic estimates (e.g. regression coefficient) AND variation (e.g. standard deviation) or associated estimates of uncertainty (e.g. confidence intervals)
- For null hypothesis testing, the test statistic (e.g. *F*, *t*, *r*) with confidence intervals, effect sizes, degrees of freedom and *P* value noted
  Give P values as exact values whenever suitable.
- For Bayesian analysis, information on the choice of priors and Markov chain Monte Carlo settings
- For hierarchical and complex designs, identification of the appropriate level for tests and full reporting of outcomes
- Estimates of effect sizes (e.g. Cohen's *d*, Pearson's *r*), indicating how they were calculated

Our web collection on statistics for biologists contains articles on many of the points above.

Software and code

Policy information about availability of computer code

Data collection	As reported in Fecher, C., Trovò, L., Müller, S.A. et al. Cell-type-specific profiling of brain mitochondria reveals functional and molecular diversity.
Data analysis	As reported in Fecher, C., Trovò, L., Müller, S.A. et al. Cell-type-specific profiling of brain mitochondria reveals functional and molecular diversity.

For manuscripts utilizing custom algorithms or software that are central to the research but not yet described in published literature, software must be made available to editors and reviewers. We strongly encourage code deposition in a community repository (e.g. GitHub). See the Nature Portfolio guidelines for submitting code & software for further information.

Data

Policy information about availability of data

All manuscripts must include a data availability statement. This statement should provide the following information, where applicable:

- Accession codes, unique identifiers, or web links for publicly available datasets
- A description of any restrictions on data availability
- For clinical datasets or third party data, please ensure that the statement adheres to our policy

This protocol does not contain custom code and data has been made available either in the original article (Fecher et al., 2019) or as supplementary information.
The MitoTag mouse line is available from The Jackson Laboratory as JAX#032675; MGI: 6296801; RRID:IMSR_JAX:032675 (Rosa26-CAG-LSL-GFP-OMM).

Human research participants

Policy information about studies involving human research participants and Sex and Gender in Research.

Reporting on sex and gender	This information has not been collected. Human research participants are not present in this protocol.
Population characteristics	This information has not been collected. Human research participants are not present in this protocol.
Recruitment	This information has not been collected. Human research participants are not present in this protocol.
Ethics oversight	This information has not been collected. Human research participants are not present in this protocol.

Note that full information on the approval of the study protocol must also be provided in the manuscript.

Field-specific reporting

Please select the one below that is the best fit for your research. If you are not sure, read the appropriate sections before making your selection.

◉ Life sciences ○ Behavioural & social sciences ○ Ecological, evolutionary & environmental sciences

Life sciences study design

All studies must disclose on these points even when the disclosure is negative.

Sample size	As reported in Fecher, C., Trovò, L., Müller, S.A. et al. Cell-type-specific profiling of brain mitochondria reveals functional and molecular diversity.
Data exclusions	As reported in Fecher, C., Trovò, L., Müller, S.A. et al. Cell-type-specific profiling of brain mitochondria reveals functional and molecular diversity.
Replication	As reported in Fecher, C., Trovò, L., Müller, S.A. et al. Cell-type-specific profiling of brain mitochondria reveals functional and molecular diversity.
Randomization	As reported in Fecher, C., Trovò, L., Müller, S.A. et al. Cell-type-specific profiling of brain mitochondria reveals functional and molecular diversity.
Blinding	As reported in Fecher, C., Trovò, L., Müller, S.A. et al. Cell-type-specific profiling of brain mitochondria reveals functional and molecular diversity.

Behavioural & social sciences study design

All studies must disclose on these points even when the disclosure is negative.

Study description	
Research sample	
Sampling strategy	
Data collection	
Timing	
Data exclusions	
Non-participation	
Randomization	

Ecological, evolutionary & environmental sciences study design

All studies must disclose on these points even when the disclosure is negative.

Study description	
Research sample	
Sampling strategy	
Data collection	
Timing and spatial scale	
Data exclusions	
Reproducibility	
Randomization	

Blinding

Did the study involve field work? Yes No

Field work, collection and transport

Field conditions

Location

Access & import/export

Disturbance

Reporting for specific materials, systems and methods

We require information from authors about some types of materials, experimental systems and methods used in many studies. Here, indicate whether each material, system or method listed is relevant to your study. If you are not sure if a list item applies to your research, read the appropriate section before selecting a response.

Materials & experimental systems

n/a	Involved in the study
	Antibodies
	Eukaryotic cell lines
	Palaeontology and archaeology
	Animals and other organisms
	Clinical data
	Dual use research of concern

Methods

n/a	Involved in the study
	ChIP-seq
	Flow cytometry
	MRI-based neuroimaging

Antibodies

Antibodies used: Name : Supplier , Catalog #, RRID , clone (lot); Dilution:

Validation: As reported in Fecher, C., Trovò, L., Müller, S.A. et al. Cell-type-specific profiling of brain mitochondria reveals functional and molecular

Eukaryotic cell lines

Policy information about cell lines and Sex and Gender in Research

Cell line source(s)

Authentication

Mycoplasma contamination

Commonly misidentified lines
(See ICLAC register)

Palaeontology and Archaeology

Specimen provenance

Specimen deposition

Dating methods

Tick this box to confirm that the raw and calibrated dates are available in the paper or in Supplementary Information.

Ethics oversight

Note that full information on the approval of the study protocol must also be provided in the manuscript.

Animals and other research organisms

Policy information about studies involving animals; ARRIVE guidelines recommended for reporting animal research, and Sex and Gender in Research

Laboratory animals	Male and female animals of the species Mus musculus/C57BL/6 (mixed N/J) background were used between 6 weeks to 6
Wild animals	Study did not involve wild animals.
Reporting on sex	Both male and female mice were used for the protocol and did not seem to affect the outcome.
Field-collected samples	Study did not involve field-collected samples.
Ethics oversight	All animal experiments were approved by the responsible regulatory agencies (Regierung von Oberbayern).

Note that full information on the approval of the study protocol must also be provided in the manuscript.

Clinical data

Policy information about clinical studies

All manuscripts should comply with the ICMJE guidelines for publication of clinical research and a completed CONSORT checklist must be included with all submissions.

Clinical trial registration	
Study protocol	
Data collection	
Outcomes	

Dual use research of concern

Policy information about dual use research of concern

Hazards

Could the accidental, deliberate or reckless misuse of agents or technologies generated in the work, or the application of information presented in the manuscript, pose a threat to:

No	Yes	
○	○	Public health
○	○	National security
○	○	Crops and/or livestock
○	○	Ecosystems
○	○	Any other significant area

Experiments of concern

Does the work involve any of these experiments of concern:

No	Yes	
○	○	Demonstrate how to render a vaccine ineffective
○	○	Confer resistance to therapeutically useful antibiotics or antiviral agents
○	○	Enhance the virulence of a pathogen or render a nonpathogen virulent
○	○	Increase transmissibility of a pathogen
○	○	Alter the host range of a pathogen
○	○	Enable evasion of diagnostic/detection modalities
○	○	Enable the weaponization of a biological agent or toxin
○	○	Any other potentially harmful combination of experiments and agents

ChIP-seq

Data deposition

☐ Confirm that both raw and final processed data have been deposited in a public database such as GEO.

☐ Confirm that you have deposited or provided access to graph files (e.g. BED files) for the called peaks.

Data access links *May remain private before publication.*	
Files in database submission	
Genome browser session (e.g. UCSC)	

Methodology

Replicates

Sequencing depth

Antibodies

Peak calling parameters

Data quality

Software

Flow Cytometry

Plots

Confirm that:

☐ The axis labels state the marker and fluorochrome used (e.g. CD4-FITC).

☐ The axis scales are clearly visible. Include numbers along axes only for bottom left plot of group (a 'group' is an analysis of identical markers).

☐ All plots are contour plots with outliers or pseudocolor plots.

☐ A numerical value for number of cells or percentage (with statistics) is provided.

Methodology

Sample preparation

Instrument

Software

Cell population abundance

Gating strategy

☐ Tick this box to confirm that a figure exemplifying the gating strategy is provided in the Supplementary Information.

Magnetic resonance imaging

Experimental design

Design type

Design specifications

Behavioral performance measures

Acquisition

Imaging type(s)

Field strength

Sequence & imaging parameters

Area of acquisition

Diffusion MRI ○ Used ○ Not used

Preprocessing

Preprocessing software

Normalization

Normalization template

Noise and artifact removal

Volume censoring

Statistical modeling & inference

Model type and settings

Effect(s) tested

Specify type of analysis: ○ Whole brain ○ ROI-based ○ Both

Statistic type for inference (See Eklund et al. 2016)

Correction

Models & analysis

n/a | Involved in the study

- Functional and/or effective connectivity
- Graph analysis
- Multivariate modeling or predictive analysis

Functional and/or effective connectivity

Graph analysis

Multivariate modeling and predictive analysis